Marine Geology 367 (2015) 171–190

Contents lists available at ScienceDirect

Marine Geology

journal homepage: www.elsevier.com/locate/margeo

# Late Pleistocene–Holocene evolution of the Doce River delta, southeastern Brazil: Implications for the understanding of wave-influenced deltas

Dilce de Fátima Rossetti [a,*], Sílvia Palloti Polizel [a], Marcelo Cancela Lisboa Cohen [b], Luiz Carlos Ruiz Pessenda [c]

[a] Division of Remote Sensing, Brazilian Institute for Space Research—INPE, São José dos Campos, SP 12245-970, Brazil
[b] Faculty of Oceanography, Federal University of Pará, Belém, PA 66075-110, Brazil
[c] Laboratório de $^{14}C$, Universidade de São Paulo, Brazil

ARTICLE INFO

*Article history:*
Received 26 January 2015
Received in revised form 15 May 2015
Accepted 26 May 2015
Available online 5 June 2015

*Keywords:*
Wave-influenced delta
Delta facies
Brazilian coast
Late Pleistocene–Holocene

ABSTRACT

Brazil's coast displays many wave-influenced deltas that are still incompletely understood, despite their significance for reconstructing the history of Late Pleistocene–Holocene sea-level changes in this region and the potential to advance in the knowledge of wave-influenced deltas. Among them, the Doce River delta is the most expressive, given its larger geographic extension. The present work shows that this is a wave-influenced delta that evolved within the context of Late Pleistocene–Holocene sea-level fluctuations, rather than a mid-Holocene lagoonal delta as proposed elsewhere. The delta had an initial progradation at an OSL age of 132.7 (±9.1) ka after the Marine Isotope Stage (MIS) 5e, which was followed by major progradation between 45,775–49,391 and 29,678–29,226 cal yr BP. Beach ridges/spits formed during these phases were in part destroyed during an ensuing transgression between 8161–7933 and 4974–4850 cal yr BP. The central delta remained dominated by fluvial processes, which kept pace with the rising sea level due to relatively high rainfall in the Doce River drainage basin. The Doce River delta started to grow again after the late-Holocene transgression, a process still on-going at the present time. During this evolution, the Doce River was deflected northward and then southward, a process that did not result in any significant facies change when the updrift and downdrift sides of the river's mouth are compared. Such a pattern is in disagreement with previously proposed asymmetry index models for wave-influenced deltas, which predict an uneven distribution of sandy- or muddy-rich deposits in the updrift and downdrift sides of the river's mouth, respectively. Several other deltas along the Brazilian coast also display facies configuration similar to the Doce River delta or have patterns opposed to those proposed by the asymmetry index models. Based on these analogs, it can be stated that the geometries and facies patterns of wave-dominated deltas are not determined simply by the interplay of fluvial and marine processes. Instead, they can be strongly influenced by the fluvial influx, sea-level changes and/or tectonic reactivations, as it appears to be the case of Brazilian wave-influenced deltas, including the Doce River delta. Such a conclusion calls for a word of caution when applying processes-based facies models to reconstruct wave-influenced deltas in the sedimentary record.


## 1. Introduction

Deltas constitute complex coastal features with highly variable sedimentary records in space and time. This depositional system has been extensively studied, which is due to economic interests, as deltaic successions can bear important hydrocarbon source rocks, and also because they allow the reconstruction of sea-level fluctuations owing to their location between the continental and marine realms (Goudie, 2004). Great progress has been made in the last decades to describe deltaic systems and establish facies models that can be useful for their recognition in the sedimentary record. Despite these efforts, the perception remains that deltas cannot be summarized into a single facies model, as numerous parameters (e.g., grain size, river-mouth processes, climate, tectonics, water depth) affect their development (see a more detailed discussion in Elliot, 2014). Among these, river-mouth processes based on a ternary diagram with fluvial-, wave- and tide-influenced end-members (Galloway, 1975) have been adopted to assess numerous modern and ancient deltas. This scheme has been useful in advancing our understanding of delta systems. However, many deltas have mixed influences (Galloway and Hobday, 1996), developing complex depositional systems in terms of morphology and facies distribution.

Hence, further studies are still needed to document various modern and ancient delta styles. In particular, wave-influenced deltas are

* Corresponding author.
*E-mail addresses:* rossetti@dsr.inpe.br (D.F. Rossetti), sppolizel@gmail.com (S.P. Polizel), mcohen80@hotmail.com (M.C.L. Cohen), pessenda@cena.usp.br (L.C.R. Pessenda).

http://dx.doi.org/10.1016/j.margeo.2015.05.012
0025-3227/

complex depositional systems with sets of prograding beach ridges having cuspate morphologies, and which are formed by sands reworked of usually river-sourced areas under wave action (e.g., Coleman and Wright, 1975; Weise, 1980; Anthony, 2015). Because of the role of waves shaping them, wave-influenced deltas share many coastal features that can be found on non-deltaic coasts, such as lagoons, bays, spits, barrier islands and strandplains (e.g., Bhattacharya and Giosan, 2003). These complications justify the need for comparing a larger number of modern and ancient deltas aiming to improve facies models and stratigraphic analyses.

Eastern Brazil has many prograding areas categorized as wave-influenced deltas, such as the deltas of São Francisco, Paraíba do Sul, Jequitinhonha and Doce rivers (Dominguez et al., 1983, 1987, Martin et al., 1987, Dominguez 1996) (Fig. 1A). Several previous publications proposed that these deltas developed by Holocene sea-level variations that probably follow global trends (Martin et al., 1993, 1996; Bittencourt et al., 2007), but a general curve which would apply to the entire Brazilian coast has long been under debate (e.g., Bittencourt et al., 1979; Suguio et al., 1985; Martin et al., 1996; Martin et al., 2003).

The Doce River delta is the largest wave-dominated delta of the Brazilian coast. The evolution of this delta has been discussed by Suguio et al. (1980), Dominguez et al. (1981) and Martin et al. (1996). In general, it was agreed that delta progradation occurred in the last 5 ka following the Holocene transgression, with its initiation in a wide lagoon. The delta would have grown through beach ridge progradation, with the latest phase occurring after 2.5 ka (Suguio et al., 1980; Dominguez et al., 1981). However, further surveys are needed to understand in more detail the evolution of the Doce River's depositional environments in space and time. Despite the overall acceptance of the lagoonal model, a previous publication (i.e., Bacoccoli, 1971) had preliminarily suggested that the Doce River could be representative of a classical model of cuspate, wave-influenced delta formed by accretion of beach ridges since its earliest stages of development, which is a proposal also worth of investigation.

The present work will focus on the Doce River delta in southeastern Brazil. In addition to contributing to the establishing of the Late Quaternary–Holocene sea-level curve along the Brazilian coast, scrutinizing the sedimentary evolution of this delta system can provide new information with potential applications to improve available facies-based models of wave-influenced deltas. Such an approach can help reconstruct the late Quaternary sea-level history along the Brazilian coast and analyze it in the context of global fluctuations. In addition, the Brazilian deltas seem to have had a complex development, consisting of beach ridges alternating with several other coastal depositional environments, such as lagoons, barrier islands, spits, and mid-ground bars and aeolian dunes (e.g., Bhattacharya and Giosan, 2003). Therefore,

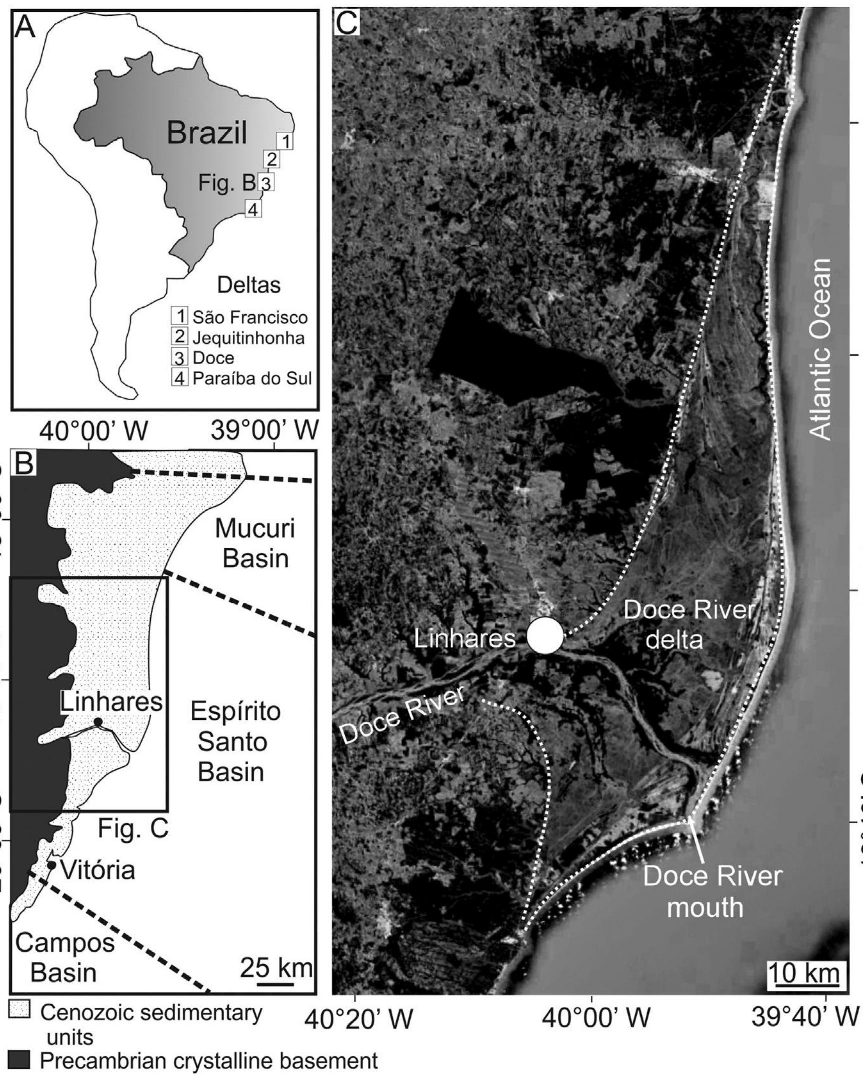


**Fig. 1.** A) Location of main deltas along the Brazilian coast, including the Doce River delta. B) Location map of the Doce River delta in the State of Espírito Santo, southeastern Brazil. C) View of the Doce River delta (dotted line) in a Google image.

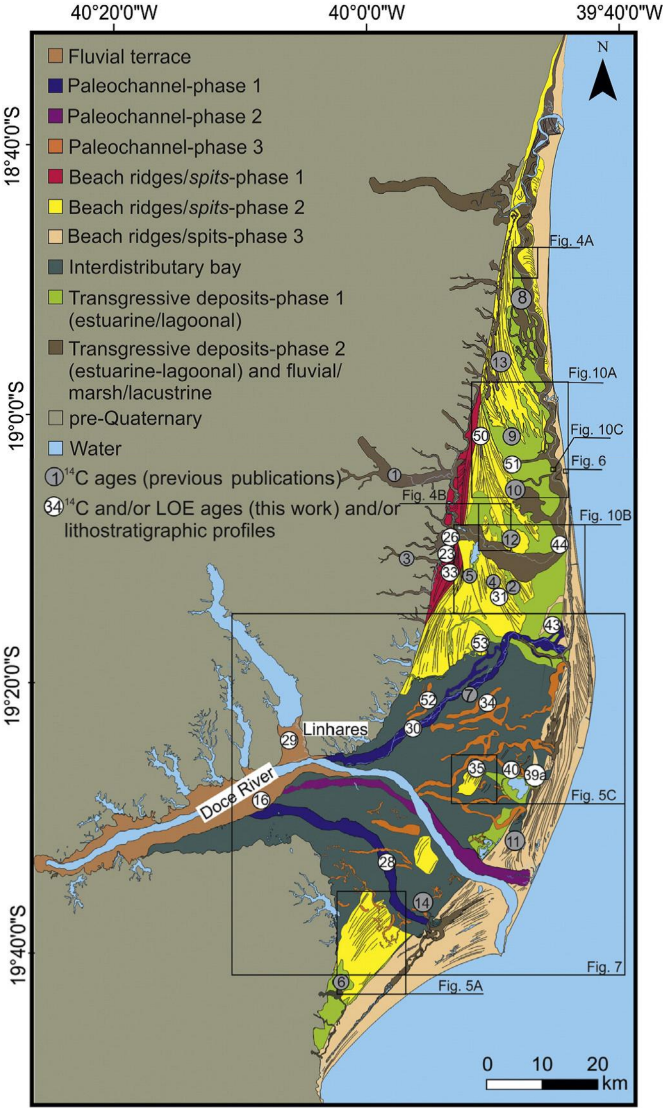


**Fig. 2.** Distribution of geomorphological units representative of depositional environments described in this work. Also included in this map are the locations of lithostratigraphic profiles, some with ages available from previous publications (Table 1) or acquired during this work (Table 2).

the examination of these deltas can provide additional data to advance our understanding about wave-influenced deltas.

## 2. Study area and geological context

The Doce River delta consists of a cuspate morphology circa 40 km wide in the E–W direction and 150 km long in the N–S direction developed in the littoral of the State of Espírito Santo, southeastern Brazil (Fig. 1). Climate in this area is tropical, classified as Aw (Köppen, 1948), with temperatures between 15 °C and 30 °C (annual mean of 22 °C). The summer is humid between November and March and the winter is dry between April and October. Prevailing waves are from the northeast, which promotes the formation of energetic waves with heights up to 2 m (Bandeira et al., 1975). The tide varies between 0.09 and 1.25 m within a semi-diurnal microtidal regime. The Doce River has a mean annual discharge of 918 $m^3 \cdot s^{-1}$ at its mouth (Coelho, 2007). Most of the sediments are deposited along the first 2 km from the river's mouth, but deposition occurs over a distance of up to 30 km offshore and at a maximum depth of 20–25 km (Summerhayes et al., 1976).

Geologically, the Doce River delta is located in the Espírito Santo–Mucuri Basin (Fig. 1), one of the Brazilian marginal rifts formed during the South Atlantic Ocean opening in the Late Jurassic and Early Cretaceous (França et al., 2007). The basin, with an onshore area of 20,000 $km^2$ and offshore area of 200,000 $km^2$, consists of Berriasian to Neoaptian synrift deposits (Millani et al., 2001; França et al., 2007). The main marine phase occurred during the Albian to Cenomanian, with transgression continuing in the late Cretaceous and Paleogene. Deposition persisted in the Neogene and Quaternary, the latter forming at the mouth of the Doce River (IBGE—Instituto Brasileiro de Geografia e Estatística, 1987), a wave-influenced delta with a series of beach ridges (Bandeira et al., 1975). Sand accumulation occurred in a valley incised into Neogene deposits (Barreiras Formation) likely developed during the Last Interglacial transgression episode circa 120 ka (Dominguez et al., 1981). The transgressive estuary thus formed was filled during delta progradation, a process that also resulted in elongated lakes or rias in replacement of several smaller estuaries along the paleocoastline (Castro et al., 2013).

## 3. Materials and methods

This work draws on the integration of previously published, as well as unpublished, geomorphological, chronological and sedimentological data. The geomorphological data was based on a modified version of the map previously documented in Polizel and Rossetti (2014). The mapping techniques, presented in detail in that publication, were based on remote sensing data including: (i) unprojected 90 m resolution digital elevation model (DEM) of the Shuttle Radar Topography Mission (SRTM) (free access in http://dds.cr.usgs.gov/srtm), resampled to 30 m pixel DEM (Valeriano et al., 2006); (ii) Phased Array type L band Synthetic Aperture Radar (PALSAR) images of the Advanced Land Observing Satellite (ALOS) from the Japan Aerospace Exploration Agency (JAXA), which consist of fine beam dual-pol HH + HV images with pixel size of 12.5 × 12.5 m, 16 bits per pixel, fixed incidence angle of 34.3° in ascending orbit, and processed in a R (red) HH G (green) HV and B (blue) HH composition; (iii) multispectral Landsat 5 Thematic Mapper (TM) optical images from the Brazilian National Institute of Space Research (INPE—Instituto Nacional de Pesquisas Espaciais, 2013) and the United State Geological Survey (USGS, 2013), with concentration of the desired information into R (red) G (green) and B (blue) color image compositions; and (iv) high resolution *GeoEye*, *RapidEye*, *Quickbird* and SPOT optical images obtained from Google Earth™ .

The remote sensing data were combined with 50 radiocarbon ages from previous publications, added to 12 $^{14}C$ and 14 optically stimulated luminescence ages (OSL) obtained during this work. Samples were from cores acquired with a manual auger and a percussion device coupled with a Cobra TT model engine and cylindrical samplers 2 m long and 6 cm in diameter. These cores also provided the basis for sedimentological descriptions including mainly lithology, texture, sedimentary structure and type of contact. The $^{14}C$ dating was achieved using an accelerator mass spectrometer (AMS) at the Beta Analytic Radiocarbon Dating Laboratory, Florida, U.S.A. A pre-treatment with acid–alkali–acid wash removed recent or ancient organic matter undergoing slow decomposition and adsorbed in the sediments. Conventional $^{14}C$ ages were calibrated to calendar years BP (cal yr BP) using CALIB 6.0 (Reimer et al., 2009). OSL analyses of quartz grains, carried out at the Laboratory of Luminescence Dating of the São Paulo State University, were performed using a blue light (470 nm) and detection through an ~5 mm Hoya U-340 filter. Thermal treatments follow the single aliquot regeneration (SAR) protocol (Murray and Wintle, 2003; Wintle and Murray, 2006). Samples were pre-heated at 200 °C during 10 s, with measurements at 125 °C during 40 s. Annual doses were calculated using U, Th, and K concentrations determined with gamma spectroscopy using an inspector portable spectroscopy workstation. The cosmic

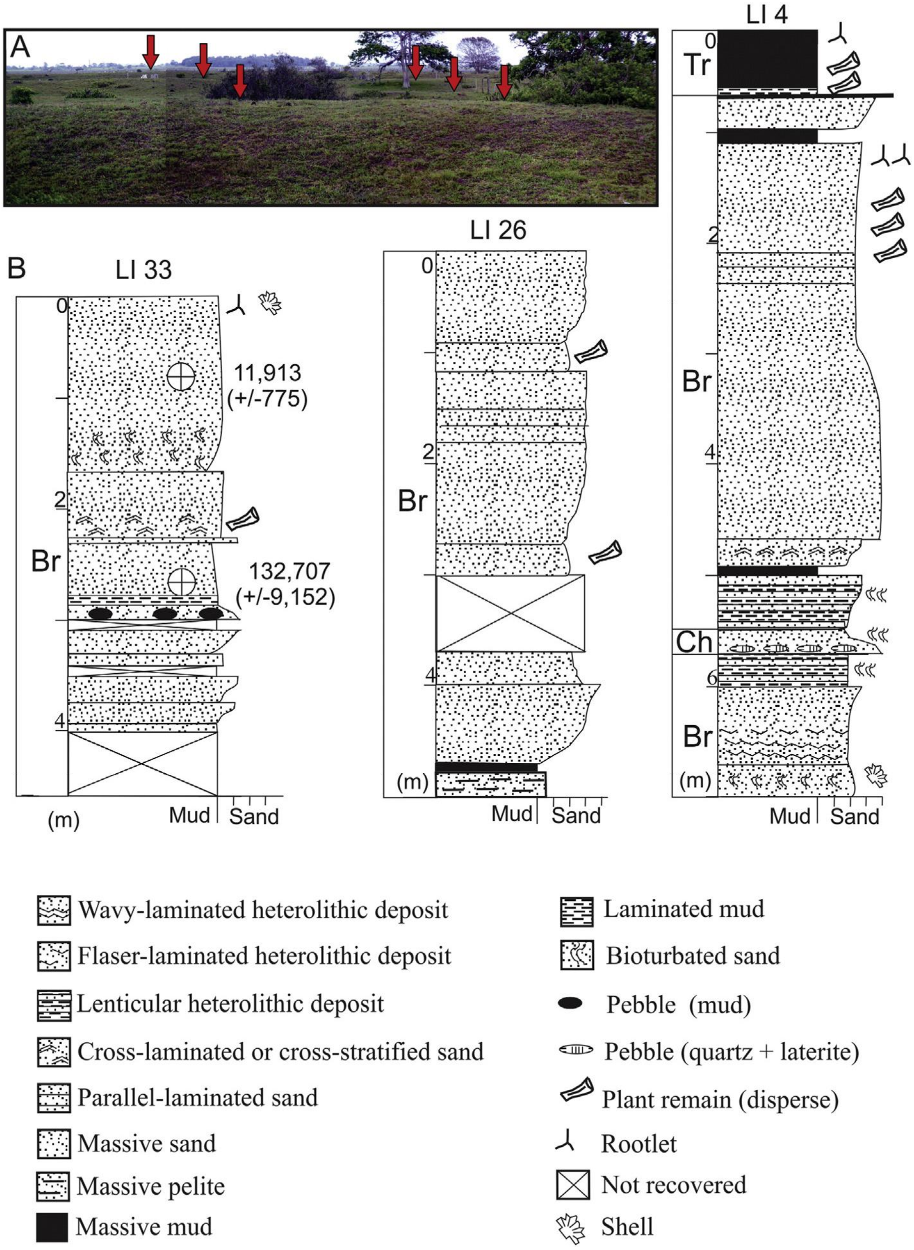


**Fig. 3.** A) Morphology of the beach ridges/spits (arrows) in the field. B) Lithostratigraphic profiles from core data on beach ridges/spits, with illustration of their sedimentary facies and related depositional environments. (Br = beach ridge/spit deposits; Ch = channel deposits; Tr = transgressive deposits). See Fig. 2 for location of the stratigraphic profiles.

radiation was calculated using the LOE-SAR age model of Prescott and Stephan (1982).

## 4. Description of geomorphological units and corresponding ages

Five geomorphological units characterize the Doce River delta plain, which correspond to surface expressions of deposits attributed to the following depositional environments (Fig. 2): 1) beach ridges/spits; 2) fluvial and distributary channels; 3) interdistributary bays; 4) transgressive (estuarine, lagoonal and embayment) environments; and 5) fluvial terraces.

### *4.1. Beach ridges/spits*

Beach ridges form elongated, narrow and convex-upward morphologies characterized by sets of parallel, either straight or gently curved lines defined by discontinuity surfaces. They are discontinuous and asymmetrically distributed along the Doce River margins, with a better development northward. In the field, beach ridges have undulating reliefs, with laterally continuous mounds (Fig. 3A) parallel to nearly parallel to the shoreline. Core data through these morphologies revealed blocky or, most often, fining- and coarsening-upward successions of massive, cross laminated/stratified or parallel-laminated or bioturbated fine to coarse-grained quartzose sands (Fig. 3B). These successions grade downward into massive or laminated mud, as well as lenticular, wavy or flaser heterolithic deposits, which are attributed to small ponds and lakes between ridges, or lagoons associated with spits. The latter are characterized in plain view by a series of parallel, curved lines perpendicular to nearly perpendicular to the coastline (Fig. 4).

Three beach ridge/spit phases were recognized in the study area. The first phase consists of an ~30 km-long and only 3 km-wide cuspate morphology with beach ridges/spits that are straight to gently convex to the east, in direct contact with the paleocoastline (see red color in Fig. 2). They are found in the central-west part of the study area, i.e., near the

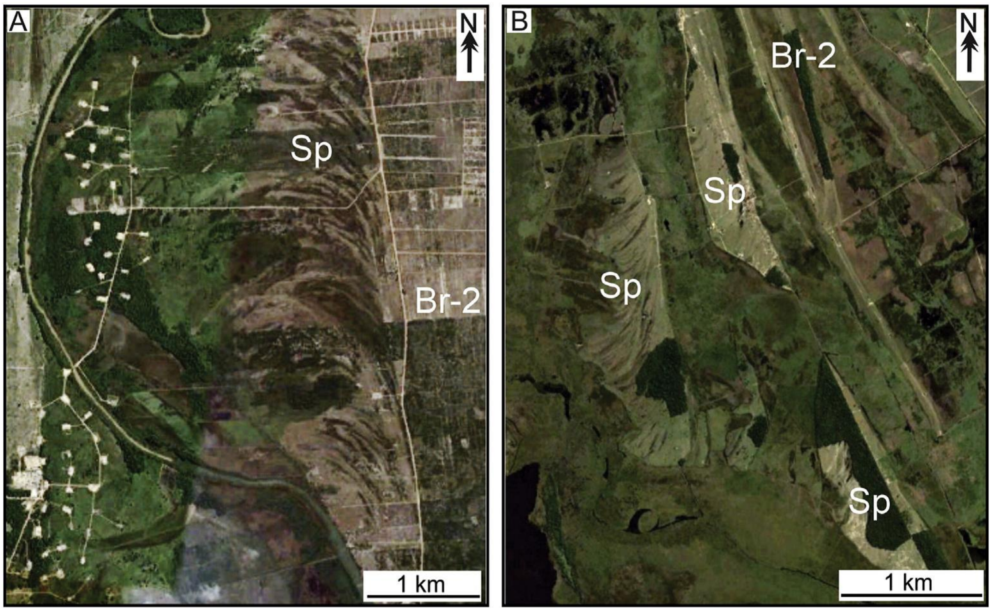


**Fig. 4.** Spit deposits associated with beach ridge deposits in the northern (A) and central areas (B) of the delta plain. Note that the spits can be recognized by a series of parallel, curved lines perpendicular to nearly perpendicular to beach ridges. (Sp = spit deposits; Br-2 = beach ridge deposits). Quickbird-Google Earth image with R3 G2 B1 composition. See location in Fig. 2.

mouth of the Barra Seca River (see location of this river in Fig. 2) approximately 50 km north of the Doce River. The chronology of these features, not as well preserved as the ones that form the rest of the delta, remains to be better established, although an OSL age of 132.7 (±9.1) ka was obtained at 2.65 m of depth (Table 1). The beach ridges/spits of phase 2 is the most representative considering both the larger extension and width, and they form a series of discontinuous belts concave to the east (yellow color in Fig. 2). The main beach ridges/spits of this phase occur northward ~40 km away from the Doce River, where they consist of three wedge-shaped sets separated by discontinuity surfaces related to successive episodes of progradation. Other beach ridges/spits of phase 2 consist of three isolated occurrences, one southeastward in the delta plain (Fig. 5A–B), and two others in the delta's center to the south and (Fig. 5C–D) north of the Doce River. All these landforms display irregular, erosional boundaries. AMS $^{14}C$ dating of organic sediments interbedded with beach ridges/spits of phase 2 recorded ages from 29,678–29,226 to 45,775–49,391 cal BP between 3.7 and 11.7 m, as previously reported by Cohen et al. (2014) (see locations 4 and 5 in Table 2). One LOE analysis (see location 31 in Fig. 3) provided the age of 31,681 years for these deposits. Beach ridges/spits of phase 3 fringe continuously the delta, forming a cuspate sand body ~160 km long and 10 km wide (beige color in Fig. 2). These features are the best preserved in the delta landscape. At 70 km northward of the Doce River mouth, the youngest beach ridge, already vegetated, and those under development stand at 6 to 7 m above the high tidal level, respectively (Fig. 6). The latter attests that delta progradation is currently active.

### 4.2. Fluvial and distributary channels

Three paleochannel morphologies intercept mainly interdistributary bay deposits (see descriptions later in this section) in the central delta (Fig. 2), where they form sinuous and elongated belts with dimensions generally similar to the modern river. The existence of these paleochannels, which converge upstream and attest previous courses of the Doce River (Fig. 7), was confirmed by core data (Fig. 8) recording highly micaceous, poorly sorted, coarse- to fine-grained sands arranged into fining-upward cycles that are sharp-based and erosional, and mantled by conglomeratic sands with abundant quartz or sandstone pebbles.

The southernmost paleochannel (phase 1), 27 km in length and 1.8 km in width, trends mainly to the southeast and ends abruptly eastward, being interrupted by beach ridges/spits of phase 3. Core data revealed a 9 m-thick fining-upward channel succession (profile 28 in Fig. 8) with OSL ages of 5.4 (±0.4) and 10.8 (±0.5) ka at depths of

**Table 1**
OSL ages of some channel and beach ridge/spit deposits of the Doce River delta area.

| Site | Paleoenvironment | Coordinate (lat S/long W) | Depth (m) | U (ppm) | Th (ppm) | K (%) | Accumulated dose (Gy) | Annual dose rate (Gy/ka) | Age (years) |
|---|---|---|---|---|---|---|---|---|---|
| 16 | Fluvial terrace | 19°27′48.56″/40°08′59.21″ | 2.10 | 1.567 | 6.364 | 0.476 | 7.67 (±0.45) | 1.42 (±0.04) | 5415 (±522) |
| 16 | Fluvial terrace | 19°27′48.56″/40°08′59.21″ | 8.60 | 0.605 | 1.771 | 0.45 | 5.89 (±0.25) | 0.68 (±0.05) | 8631 (±731) |
| 16 | Fluvial terrace | 19°27′48.56″/40°08′59.21″ | 14.12 | 0.585 | 2.421 | 0.431 | 4.96 (±0.28) | 0.66 (±0.05) | 7522 (±697) |
| 28 | Channel | 19°32′00.56″/39°58′12.22″ | 0.80 | 0.872 | 4.628 | 0.625 | 6.71 (±0.04) | 1.25 (±0.09) | 5395 (±401) |
| 28 | Channel | 19°32′00.56″/39°58′12.22″ | 2.30 | 0.927 | 4.005 | 0.685 | 8.09 (±0.04) | 0.75 (±0.03) | 10,771 (±460) |
| 29 | Fluvial terrace | 19°23′10.79″/40°06′03.74″ | 0.55 | 2.378 | 11.296 | 0.763 | 9.77 (±0.32) | 2.04 (±0.14) | 4800 (±368) |
| 29 | Fluvial terrace | 19°23′10.79″/40°06′03.74″ | 2.70 | 0.789 | 2.555 | 0.516 | 5.97 (±0.16) | 0.94 (±0.07) | 6322 (±495) |
| 29 | Fluvial terrace | 19°23′10.79″/40°06′03.74″ | 7.35 | 0.604 | 2.510 | 0.644 | 7.84 (±0.18) | 0.89 (±0.07) | 8765 (±677) |
| 30 | Channel | 19°21′48.51″/39°55′52.43″ | 0.57 | 0.652 | 2.766 | 0.479 | 5.76 (±0.20) | 1.00 (±0.08) | 5753 (±489) |
| 30 | Channel | 19°21′48.51″/39°55′52.43″ | 2.70 | 0.592 | 1.911 | 0.489 | 4.83 (±0.25) | 0.76 (±0.05) | 6330 (±541) |
| 30 | Channel | 19°21′48.51″/39°55′52.43″ | 4.90 | 0.581 | 2.097 | 0.437 | 4.46 (±0.28) | 0.78 (±0.06) | 5703 (±566) |
| 31 | Beach ridge/spit | 19°27′48.56″/40°08′59.21″ | 3.85 | 1.948 | 11.840 | 0.622 | 59.34 (±4.11) | 1.87 (±0.14) | 31,681 (±3203) |
| 33 | Beach ridge/spit[a] | 19°10′19.16″/39°53′10.72″ | 0.80 | 0.473 | 1.093 | 0.040 | 4.30 (±0.04) | 0.36 (±0.02) | 11,913 (±775) |
| 33 | Beach ridge/spit | 19°10′19.16″/39°53′10.72″ | 2.65 | 0.195 | 1.720 | 0.157 | 56.63 (±0.36) | 0.43 (±0.03) | 132,705 (±9152) |

[a] Reworked.

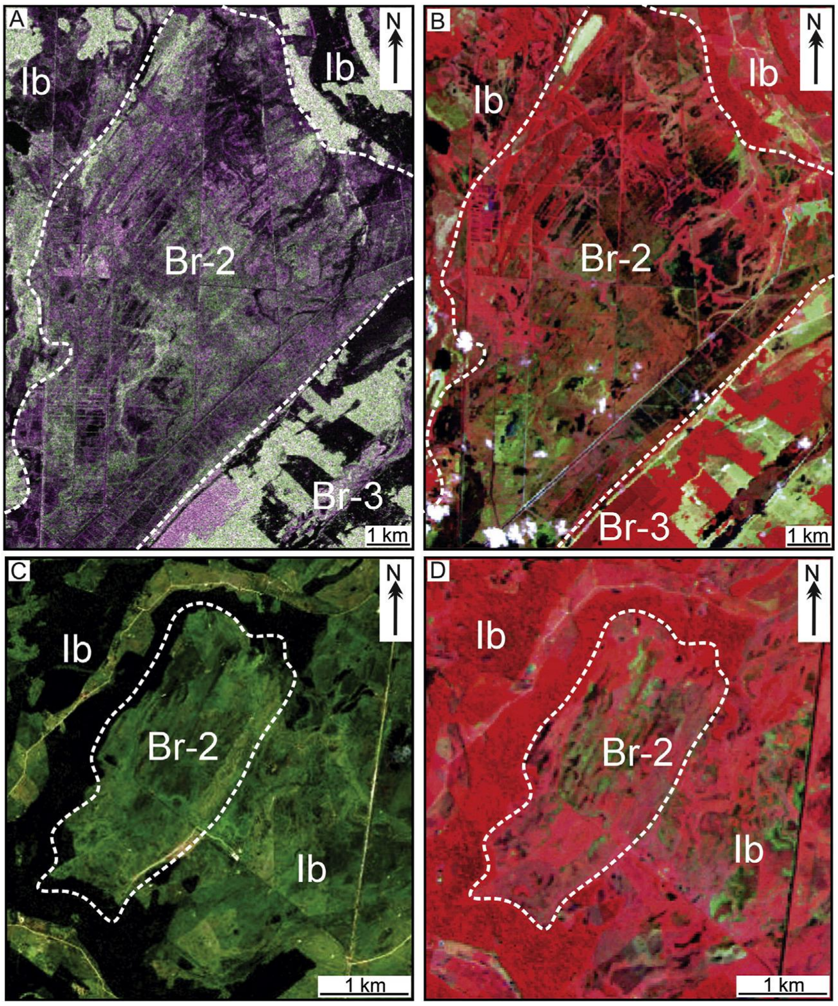


**Fig. 5.** Isolated bodies of a beach ridge/spit of phase 2 (Br-2) within interdistributary bay deposits (Ib), which demonstrate the continuity of delta progradation during phase 2 in the southern (A–B) and central (C–D) areas of the delta plain. A = PALSAR image with RHH GHV BHH composition; B, D = TM Landsat images with R4 G7 B2 compositions; C = Quickbird-Google Earth image with R3 G2 B1 composition. See location in Fig. 2.

0.80 and 2.30 m, respectively (see Table 1 and profile 28 in Fig. 8). A more extensive (i.e., ~40 km long) and sinuous, although narrower (1 km wide in average), paleochannel occurs to the north of the Doce River (phase 2). This feature bifurcates downstream in its middle course, configuring a distributary network. Downstream, it turns orthogonally from northeast to southeast, cutting down into transgressive deposits of phase 1 (see later descriptions), as well as through beach ridges/spits of phase 3, although it intercepts a few of these features at the delta's fringe. This northernmost paleochannel is superimposed by a network of active narrow channels. A third paleochannel is represented by a belt nearly 45 km long and 1.5 km wide that occurs nearly parallelling the east to southeast course of the modern Doce River. The latter intercepts the paleochannel in its medium course. Downstream, this paleochannel cuts through beach ridges/spits of phase 3, ending just westward of a few beach ridges/spits, while the modern river deflects southward to follow a course nearly parallel to the coastline before discharge into the Atlantic Ocean (Fig. 2).

The central delta is also intercepted by a myriad of small paleochannels of a distributary network. Some of these paleochannels intercept the westernmost beach ridges/spits of phase 3. A few of them deviate around an island of beach ridges/spits of phase 2. In the field, areas corresponding to paleochannels are sandy, while adjacent areas, mainly composed of interdistributary bay deposits, essentially consist of mud and organic matter. Morphologically, the paleochannels can be either slightly convex-up or concave-up, depending on the stage of abandonment. The former are likely older and result from differential compaction of sands, which are less compactable than surrounding muds related to interdistributary bay areas.

### *4.3. Interdistributary bay*

Areas related to interdistributary bays dominate the central delta plain, where they correspond to extensive fan-shaped deposits nearly 60 km in radius (Fig. 2). An important characteristic is their close association with the paleochannel morphologies (Figs. 2 and 9A). Interdistributary bay deposits are intercepted by fluvial terraces to the west, while they intercept beach ridges/spits of phase 2 to the north and south (Fig. 2). In the latter instance, the contact of these deposits is typically sharp and erosional, with interdistributary bay deposits advancing toward beach ridge/spit deposits. To the east, bay deposits are either bounded or cut through transgressive deposits of phase 1 (see descriptions below). They can also be in direct contact with beach ridges/spits of phase 3, locally developing over them.

In addition to their spatial distribution and relationship with the other geomorphological units, areas corresponding to interdistributary bays were characterized in the field by extensive flat-lying areas of either massive or laminated muds (Fig. 9B). These are generally highly organic and grade laterally into muddy peats. Circular areas of mud and peat deposits at the surface were related to lakes within interdistributary bays. Cores attest to the continuity of mud and peat deposits in the

**Table 2**
Radiocarbon ages for deposits in the Doce River delta compiled from previous publications.

| Site | Paleoenvironment[a] | Coordinate (lat-S/long-W) | Depth (m) | Cal yr BP 2-sigma calibration (AMS) | Reference |
|---|---|---|---|---|---|
| 1 | Lake-marsh | 19°02′58.40″/39°56′69.50″ | 0.48–0.50 | 253–0.00 | Buso et al. (2013) |
| 1 | Lake-marsh | 19°02′58.40″/39°56′69.50″ | 0.64–0.66 | 440–154 | |
| 1 | Lake-marsh | 19°02′58.40″/39°56′69.50″ | 0.68–0.70 | 1171–767 | |
| 1 | Transgressive phase 2 (fluvio-estuarine) | 19°02′58.40″/39°56′69.50″ | 0.72–0.74 | 1348–1190 | |
| 1 | Transgressive phase 2 (fluvio-estuarine) | 19°02′58.40″/39°56′69.50″ | 0.76–0.78 | 2717–2208 | |
| 1 | Transgressive phase 2 (fluvio-estuarine) | 19°02′58.40″/39°56′69.50″ | 0.80–0.82 | 3479–3361 | |
| 1 | Transgressive phase 2 (fluvio-estuarine) | 19°02′58.40″/39°56′69.50″ | 0.92–0.94 | 4238–3992 | |
| 1 | Transgressive phase 1 (estuarine) | 19°02′58.40″/39°56′69.50″ | 1.08–1.10 | 5431–4888 | |
| 1 | Transgressive phase 1 (estuarine) | 19°02′58.40″/39°56′69.50″ | 1.22–1.24 | 5571–4858 | |
| 1 | Transgressive phase 1 (estuarine) | 19°02′58.40″/39°56′69.50″ | 1.26–1.28 | 6293–6024 | |
| 1 | Transgressive phase 1 (estuarine) | 19°02′58.40″/39°56′69.50″ | 1.34–1.36 | 6634–6414 | |
| 1 | Transgressive phase 1 (estuarine) | 19°02′58.40″/39°56′69.50″ | 1.38–1.40 | 7159–6694 | |
| 1 | Transgressive phase 1 (estuarine) | 19°02′58.40″/39°56′69.50″ | 1.70–1.72 | 7458–7172 | |
| 1 | Transgressive phase 1 (estuarine) | 19°02′58.40″/39°56′69.50″ | 1.98–2.00 | 7667–7430 | |
| 2 | Lacustrine | 19°11′36.67″/39°48′16.56″ | 0.67–0.72 | 3246–2840 | França et al. (2013) |
| 2 | Transgressive deposits phase 1 | 19°11′36.67″/39°48′16.56″ | 1.40–1.45 | 7278–6955 | |
| 2 | Transgressive deposits phase 1 | 19°11′36.67″/39°48′16.56″ | 3.40–3.45 | 7318–7172 | |
| 2 | Transgressive deposits phase 1 | 19°11′36.67″/39°48′16.56″ | 4.30–4.35 | 7339–7259 | |
| 2 | Transgressive deposits phase 1 | 19°11′36.67″/39°48′16.56″ | 5.45–5.50 | 8161–7933 | |
| 3 | Marsh/fluvial channel | 19°09′08.46″/39°55′53.50″ | 1.00 | Modern | Castro et al. (2013) |
| 3 | Marsh/fluvial channel | 19°09′08.46″/39°55′53.50″ | 3.00 | 1405–1313 | |
| 3 | Transgressive phase 1 | 19°09′08.46″/39°55′53.50″ | 5.00 | 5201–5047 | |
| 3 | Transgressive phase 1 | 19°09′08.46″/39°55′53.50″ | 6.70 | 7317–7171 | |
| 3 | Transgressive phase 1 | 19°09′08.46″/39°55′53.50″ | 9.50 | 7509–7425 | |
| 4 | Lacustrine | 19°11′16.26″/39°49′32.52″ | 1.05–1.10 | 4845–3933 | Cohen et al. (2014) |
| 4 | Beach ridge phase 2 | 19°11′16.26″/39°49′32.52″ | 6.55–6.65 | 30,465–31,022 | |
| 5 | Transgressive phase 1 | 19°10′52.90″/39°51′54.54″ | 1.65–1.75 | 7556–7622 | Cohen et al. (2014) |
| 5 | Distributary channel | 19°10′52.90″/39°51′54.54″ | 3.70–3.75 | 29,226–29,678 | |
| 5 | Beach ridge/spit phase 2 | 19°10′52.90″/39°51′54.54″ | 6.20–6.30 | 36,105–40,014 | |
| 5 | Beach ridge/spit phase 2 | 19°10′52.90″/39°51′54.54″ | 8.80–8.86 | 35,162–36,321 | |
| 5 | Beach ridge/spit phase 2 | 19°10′52.90″/39°51′54.54″ | 11.52–11.70 | 45,775–49,391 | |
| 6 | Transgressive phase 1 | – | – | 6802–5934 | Suguio et al. (1982) |
| 6 | Transgressive phase 1 | – | – | 7158–6268 | |
| 6 | Transgressive phase 1 | – | – | 7265–6273 | |
| 6 | Transgressive phase 1 | – | – | 7423–6394 | |
| 6 | Transgressive phase 1 | – | – | 7505–6462 | |
| 6 | Transgressive phase 1 | – | – | 7509–6675 | |
| 6 | Transgressive phase 1 | – | – | 7565–6731 | |
| 6 | Transgressive phase 1 | – | – | 7592–6781 | |
| 7 | Interdistributary bay | – | – | 5324–4242 | Suguio et al. (1982) |
| 8 | Transgressive phase 1 | – | – | 6790–5909 | Suguio et al. (1982) |
| 8 | Transgressive phase 1 | – | – | 7314–6413 | |
| 9 | Transgressive phase 2 ? | – | – | 3581–2860 | Suguio et al. (1982) |
| 9 | Transgressive phase 2 ? | – | – | 4238–3455 | |
| 10 | Transgressive phase 2 | – | – | 4000–3004 | Suguio et al. (1982) |
| 11 | Interdistributary bay | – | – | 4877–3829 | Suguio et al. (1982) |
| 12 | [b] | – | – | 5332–4778 | Suguio et al. (1982) |
| 13 | Transgressive phase 2 | – | – | 3514–2754 | Suguio et al. (1982) |
| 13 | [b] | – | – | 5092–4420 | |
| 14 | Interdistributary bay 1 | – | – | 4090–3360 | Suguio et al. (1982) |

(–) data not available in the corresponding reference.
[a] Interpretation provided by this work.
[b] Sambaqui on beach ridge/spit.

shallow subsurface (Fig. 9C), which overlie distributary channel and beach ridge/spit deposits. AMS dating of organic matter from bay muds recorded ages ranging from 6894–6737 to 4090–3360 cal yr BP (Tables 2 and 3).

### 4.4. Transgressive deposits

Transgressive deposits form a belt that is continuous over a great part of the delta plain, being discontinuous in the central delta (Fig. 2). They are located between beach ridges/spits of phase 2 (Fig. 10A, B), between these and beach ridges/spits of phase 3 or, in the case of the central delta, between the latter and interdistributary bay deposits. In the field, areas related to transgressive deposits are indicated either by partly flooded and elongated depressions consisting mainly of marshes, or dry areas with mud and muddy peats (Fig. 10C). Although similar to interdistributary bay deposits, the transgressive lithologies display locally abundant shell fragments (Fig. 10D). In addition, they grade downward into wavy and lenticular heterolithic deposits and either massive or parallel-laminated sands arranged into sharp-based fining upward cycles. These sands, which have quartz pebbles at their bases, are generally better sorted and not as micaceous as sands associated with channel deposits, and they contain locally abundant shell fragments. In addition, transgressive deposits are surrounded by beach ridge/spit morphologies.

Two transgressive phases were distinguished (Fig. 2). The main one is represented by deposits that start ~35 km northward of the Doce River and extend up to the delta's northernmost margin. These deposits advance into beach ridges/spits of phase 2 (Fig. 10A) to form ragged contacts or even elongated tongues more than 10 km in length that extend parallel to the ridge and swale morphology. In some locations, they advanced westward and cut through the entire belt of beach ridges/spits. At certain places, this process resulted in islands of beach ridges/spits within the transgressive deposits. The transgression advanced or crossed over the paleoshoreline to influence a series of estuarine systems that cut

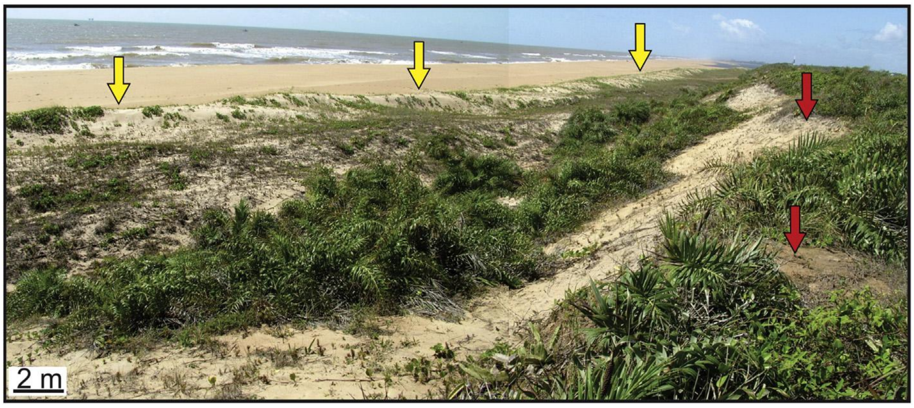


**Fig. 6.** View of the newest beach ridges formed in the Doce River delta plain. Note a higher and more vegetated beach ridge to the right (red arrows) and the lower and almost non-vegetated beach ridge (yellow arrows) that stands parallel to the coastline. (For interpretation of the references to color in this figure legend, the reader is referred to the web version of this article.)

down into the Miocene Barreiras Formation. Transgressive deposits of phase 1 also form isolated bodies in front of interdistributary bay deposits to the north of the Doce River in the central delta, some with funnel-shaped morphologies partly occupied by modern lakes (see these features near locations 39a and 40 in Fig. 2). The southernmost end of the delta also records transgressive deposits of phase 1 as a wedge-shaped morphology nested between the paleoshoreline and the beach ridges/spits of phase 2 or 3. AMS dating of plant debris from muds and peats of transgressive deposits of phase 1 recorded ages between 8161–7933 and 4974–4850 cal yr BP (Tables 2 and 3).

A younger transgressive phase was recognized by a series of elongated and narrow belts that range from straight to sinuous or even meandering. These features, which cut down through transgressive deposits of phase 1 to the north of the Doce River, encompasses a narrow (i.e., usually b2 km in width) but extensive (i.e., 70 km long), N–S trending belt that parallels the coastline along most of its extension. It continues northward up to the limit of the delta system, where it intercepts beach ridges/spits of phase 2. Southward, this belt enlarges to a width of up to 5 km as it turns orthogonally to E–W to cut transversally through beach ridges/spits of phases 2 (Fig. 10B). It also cuts through beach ridges/spits of phase 3, extending to the north and south. Transgressive deposits of phase 2 are also composed of several narrow, either sinuous or essentially straight and elongated bodies parallel to sub-parallel to the beach ridges/spits of phase 3. A few of these features also intercept transgressive deposits of phase 1 in the southernmost end of the delta plain. These channelized deposits, mainly estuarine in nature, are transitional to modern/sub-modern marsh and fluvial systems. AMS dating of plant debris from muds and peats of transgressive deposits of phase 2 recorded ages between 4238–3992 and 537–484 cal yr BP (Tables 2 and 3).

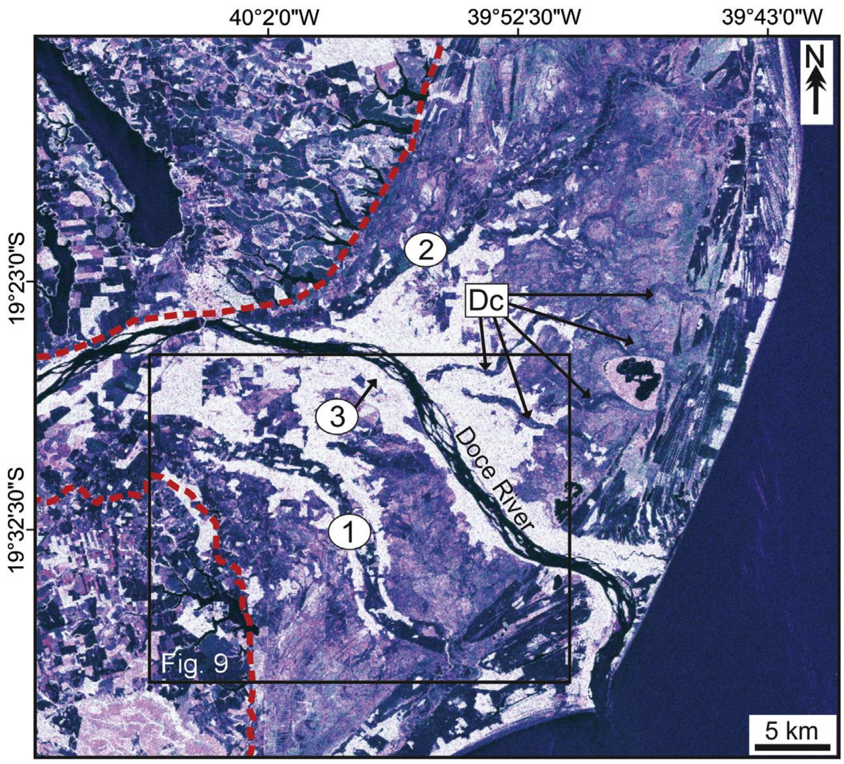


**Fig. 7.** PALSAR image with a RHH GHV BHH composition, illustrating paleochannels (1 to 3) attributed to previous locations of the Doce River delta. In addition to these major paleochannels, a myriad of smaller-size paleochannels related to a distributary network (Dc) were mapped in the delta plain. (Red hatched line = paleocoastline). See location in Fig. 2.

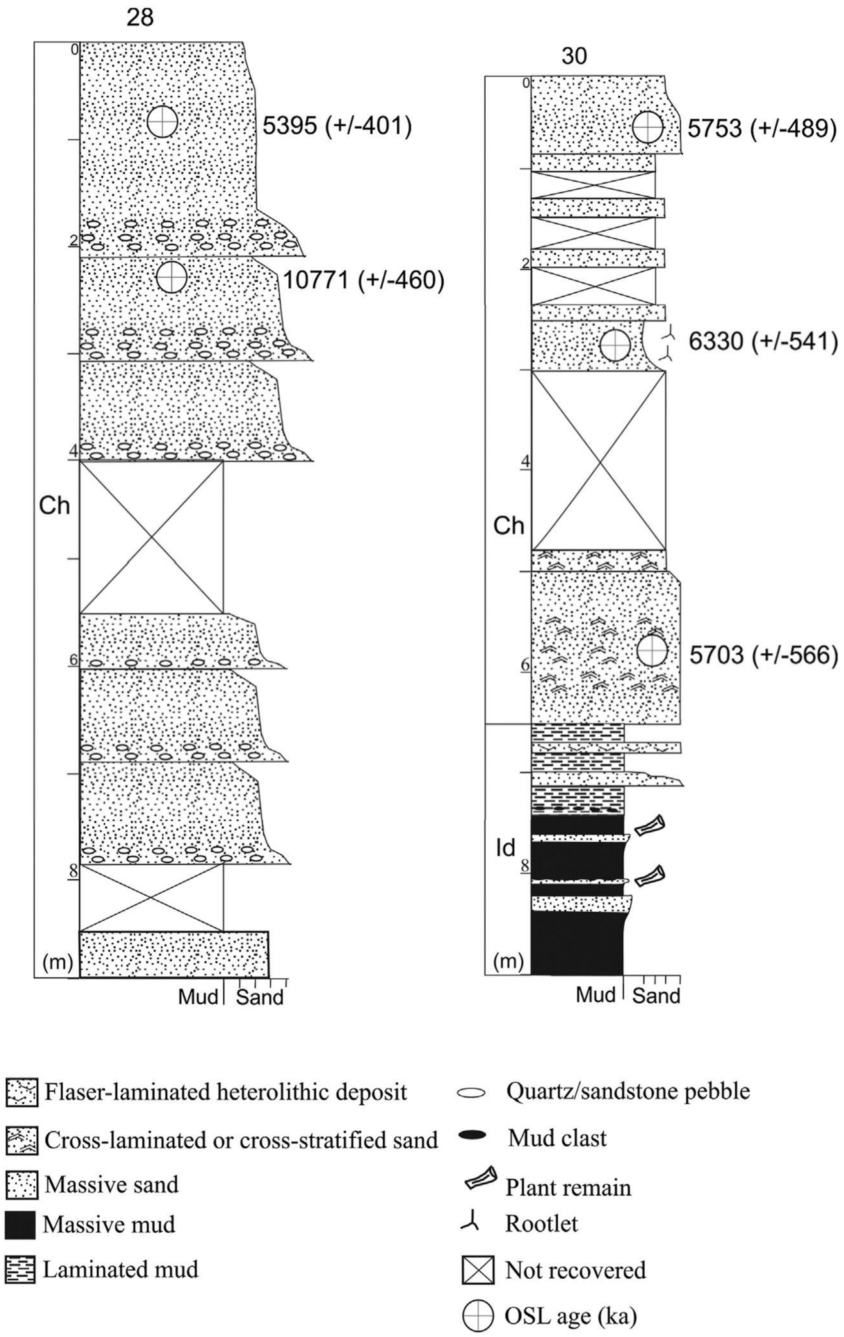


**Fig. 8.** Lithostratigraphic profiles derived from core data representative of the vertical distribution of sedimentary facies in channel deposits, which correspond to previous courses of the Doce River along the central delta plain. See location in Fig. 2.

### *4.5. Fluvial terraces*

Fluvial terraces were recorded along the innermost delta plain on both sides of the Doce River. These features form elongated belts up to 60 km long and less than 5 km wide. The fluvial terrace located at the left (northern) margin of the river is in direct contact with the Barreiras Formation. It presents several elongated lakes or fluvial rias (i.e., ancient fluvial systems that were barred by the deposition of fluvial terraces). The fluvial terrace at the right (southern) margin of the Doce River is in sharp contact with areas related to interdistributary bays. It also truncates the three paleochannels related to previous courses of the Doce River. LOE ages obtained from these fluvial terrace deposits recorded several ages between 8.8 (±0.7) and 4.8 (±0.4) ka (Table 1).

## 5. Discussion

The data presented here allow questioning the lagoonal delta model and the Holocene age of the Doce River delta proposed in previous publications. These data are also used to discuss the delta's evolution within the context of relative sea-level and climatic changes. In addition, observations derived from this delta and comparisons with other deltas from the Brazilian coast call for a revisit of facies patterns predicted by available wave-influenced delta models.

### *5.1. Analysis of delta type*

The data presented here suggest a depositional model for the Doce River delta that differs from the previously proposed lagoonal type

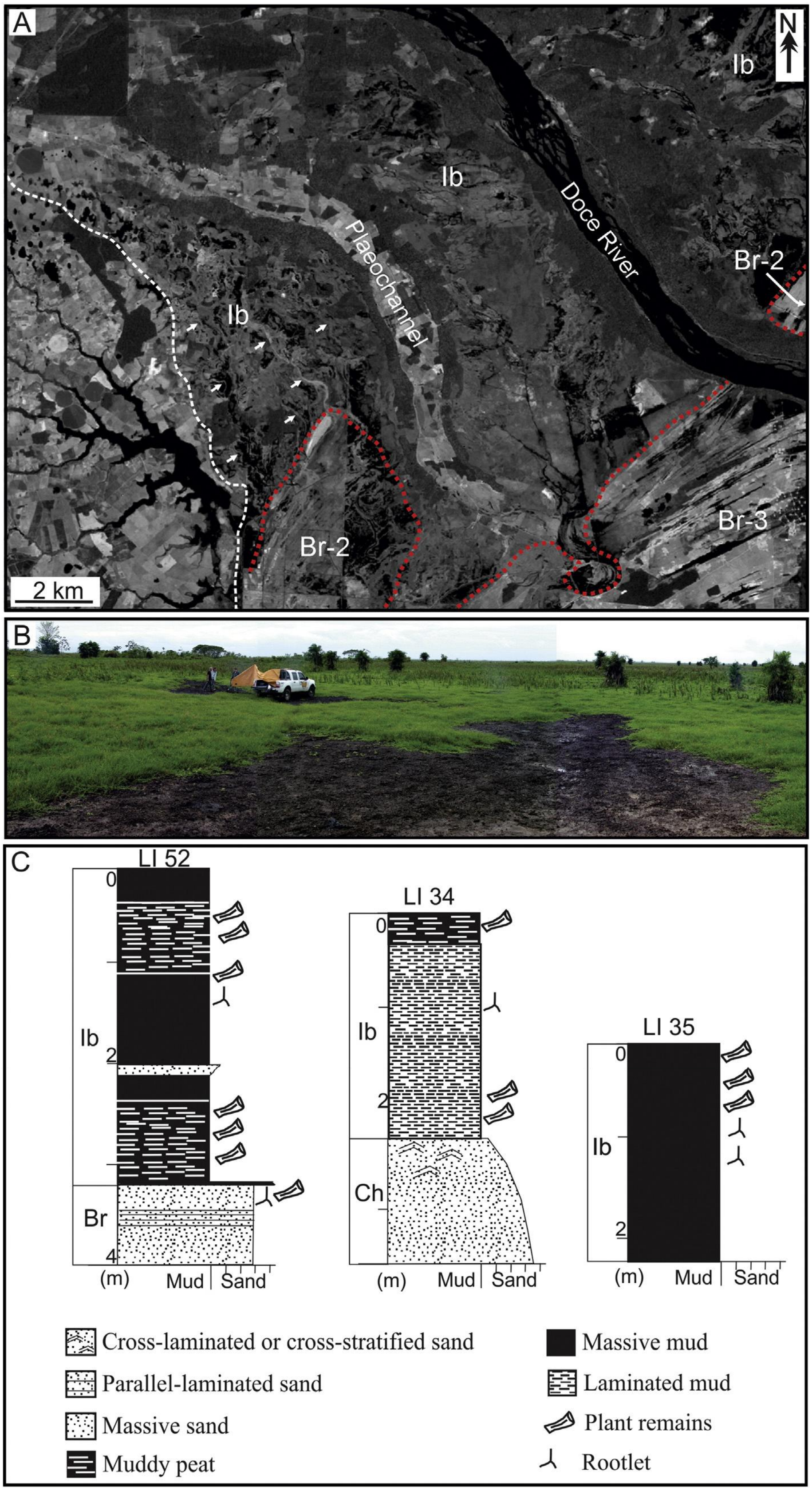


**Fig. 9.** Interdistributary bay deposits. A) PALSAR image with a RHH GHV BHH composition, illustrating the areas related to interdistributary bays (Ib). Note the surface of these deposits, which is dominated by channeling (arrows). Beach ridges of phases 2 (Br-2) and 3 (Br-3) are also shown in this figure. See location in Fig. 7. B) Field view of interdistributary bay deposits, which correspond to depressed areas dominated by organic muds and pits. C) Lithostratigraphic profiles derived from core data representative of the vertical distribution of sedimentary facies. See Fig. 2 for location.

**Table 3**
Radiocarbon ages for deposits in the Doce River delta obtained during this work.

| Locality | Paleoenvironment | Coordinate (lat S/long W) | Depth (m) | $^{14}$C yr BP measured | Cal yr BP 2-sigma calibration (AMS) |
|---|---|---|---|---|---|
| 34 | Interdistributary bay | 19°20′10.82″/39°49′52.68″ | 2.20 | 4870 (±30) | 5623–5578 |
| 35 | Interdistributary bay | 19°25′07.21″/39°51′00.61″ | 2.18 | 5810 (±30) | 6732–6554 |
| 40 | Transgressive phase 1 | 19°25′49.58″/39°47′27.31″ | 4.10 | 6680 (±30) | 7574–7460 |
| 43 | Transgressive phase 1 | 19°14′36.92″/39°44′55.07″ | 2.10 | 4350 (±30) | 4850–4974 |
| 44 | Transgressive phase 2 | 19°08′20.72″/39°43′43.39″ | 1.70 | 2950 (±30) | 3001–3183 |
| 44 | Transgressive phase 2 | 19°00′17.71″/39°50′34.08″ | 3.55 | 3080 (±30) | 3350–3174 |
| 50 | Transgressive phase 2 | 19°00′17.71″/39°50′34.08″ | 4.00 | 470 (±30) | 537–484 |
| 51 | Transgressive phase 2 | 19°02′34.26″/39°48′09.47″ | 1.15 | 910 (±30) | 733–834 |
| 51 | Transgressive phase 2 | 19°02′34.26″/39°48′09.47″ | 4.95 | 2430 (±30) | 2491–2346 |
| 52 | Interdistributary bay | 19°20′07.51″/39°55′07.03″ | 0.90 | 3060 (±30) | 3206–3359 |
| 52 | Interdistributary bay | 19°20′07.51″/39°55′07.03″ | 310 | 6040 (±30) | 6894–6737 |
| 53 | Interdistributary bay | 19°15′41.44″/39°50′47.87″ | 2.65 | 5660 (±30) | 6454–6313 |

(e.g., Suguio and Martin, 1981; Dominguez et al., 1987). Sediment progradation in an open marine setting since the earliest stage of the delta evolution is supported by the beach ridges/spits over the entire delta plain, even in the central area where previous interpretations reported lagoon deposits. Beach ridges/spits in a deltaic system originate from longshore drift of mainly fluvial-sourced sediment due to wave action. Therefore, the occurrence of such deposits in the central delta is inconsistent with a wide lagoon where the delta would have prograded, as no beach ridges are expected to form in backbarrier lagoonal areas, generally protected from wave action. The close association of bay deposits with paleochannels of the Doce River or distributary channels indicates that the muddy and peat deposits of the central delta are related to interdistributary bays, rather than to a lagoon. The isolated occurrences of beach ridges/spits of phase 2 within interdistributary bay deposits are consistent with the continuous formation of the former on both sides of the feeding river. Only later were beach ridges/spits eroded from the central delta area due to channel development and migration. In addition, part of the beach ridges/spits was buried due to deposition of interdistributary bay deposits.

Further evidence against the lagoonal model includes the lack of any corresponding barrier that could have confined the proposed semi-enclosed water body in the central delta. Such a barrier would have to be recorded to the east of the supposed lagoon deposits. Instead, beach ridges/spits of phase 3 are identified at that location. These are the best preserved beach ridges/spits of the entire delta, with well-preserved morphologies that allow them to be promptly recognized in remote sensing products. Thus, they are related to the latest stage of delta progradation, as discussed below, an interpretation not compatible with an earlier barrier growth associated with the hypothesized lagoon.

## 5.2. Delta evolution

The geomorphological data, analyzed within a chronological context based on the ages provided here and in previous publications, support the idea that the Doce River delta was built by alternating episodes of progradation and transgression in overall agreement with the sea-level history from several other areas worldwide (Fig. 11). Hence, the first stage of delta development occurred at approximately 50 km to the north of the modern Doce River (Fig. 12A), being recorded by the beach ridges/spits of phase 1 (Fig. 12B). Whether such deposits were fed by sediments sourced from the Doce River or a nearby drainage system, for instance the Barra Seca River, is unknown. Although the time when these deposits began to accumulate is also unknown, it is noteworthy that they indicate the active formation of beach ridges/spits in this region starting at 132 ka. During this time, there was no delta progradation linked directly to the Doce River mouth, where an estuary was under development (cf. Dominguez et al., 1981).

The beach ridges/spits of phase 2 are most likely related to a much more widespread delta progradation (Fig. 12C). It was proposed that the onset of this event occurred at ~6 ka (e.g., Bandeira et al., 1975; Suguio et al., 1980; Dominguez et al., 1987; Martin et al., 1996), but the ages between 45,775–49,391 and 29,678–29,226 cal yr BP (Table 2) of muddy deposits interbedded with these beach ridges/spits, and the OSL age of ~31.4 ka derived from beach ridge sands at locality 31 (Table 1), suggest progradation still in the Late Pleistocene. This interpretation is compatible with two OSL ages of 5395 and 10,771 yr BP at the respective depths of 0.80 and 2.30 m (Table 1) obtained for the southward paleochannel of the Doce River, which yield an estimated age of nearly 40,000 yr BP for the basal deposits of this channel succession (assuming constant sedimentation rates). It follows that the beach ridges/spits of phase 2 were probably formed by sediment transported to the coast through this channel, since the age of these deposits are comparable. Therefore, the Doce River likely occupied a southern position (Fig. 12C) during the main phase of delta progradation in the Late Pleistocene, transporting a large volume of sediments that were deposited at its mouth and subsequently redistributed alongshore to form beach ridges/spits on the entire extension of the delta plain.

Subsequent to the main phase of progradation in the Late Pleistocene, the existing older beach ridges and other deltaic deposits were partly reworked between 8161–7933 and 4974–4850 cal yr BP (e.g., Buso et al., 2013; Castro et al., 2013; França et al., 2013; Cohen et al., 2014) (Fig. 12D), as indicated by transgressive deposits related to embayments, estuaries and lagoons that overlie a large portion of the beach ridges/spits of phase 2. This event reached far westward and even crossed the paleoshoreline, ultimately flooding underfilled estuaries previously abandoned over the Barreiras Formation in the continental area (Fig. 12C, D). These estuaries displayed sedimentary records indicating brackish conditions up to the mid-Holocene, when these water bodies gradually became completely continental-influenced as documented earlier (i.e., Castro et al., 2013; Buso et al., 2013; França et al., 2013; Cohen et al., 2014).

A second transgressive episode is suggested by estuarine and lagoon deposits formed between 4238–3992 and 537–484 cal yr BP (Tables 2 and 3). The occurrence of transgressive deposits of phase 2 parallel to subparallel to beach ridges/spits of phase 3 may suggest alternating periods of transgression and progradation.

The fact that the transgressive deposits are less expressive and more discontinuous in the central delta is probably due to the strong influence of fluvial influx. The ages obtained for the top of the southernmost paleochannel succession (i.e., 5.4 ka), as well as for the northernmost paleochannel, indicate that they are in part coeval with the transgressive deposits. This, together with the fact that the paleochannels cut through the latter deposits, indicates that the channel remained active during and after the transgression.

While the Doce River occupied a northernmost position, it appears that the delta either did not grow or underwent limited development. Although not distinguished in the map of Fig. 2, the innermost beach ridges/spits of phase 3 at this location could have been formed by sediment brought into the coast while the river occupied this position. The position of the Doce River changed again to occupy a more central

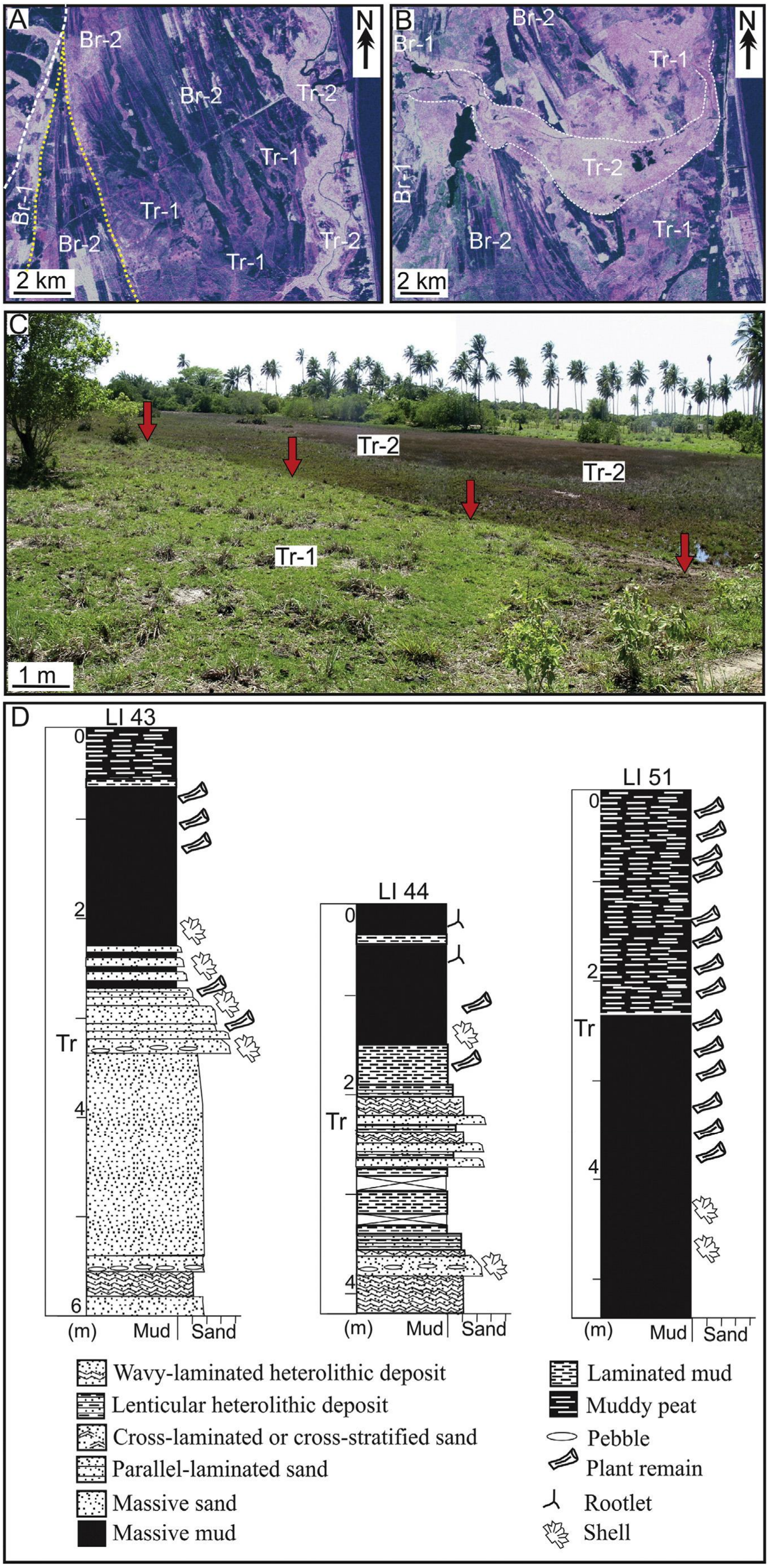
A
Br-2
Br-2
Tr-2
Tr-1
Br-1
Tr-1
Br-2
Tr-2
Tr-1
2 km
N
B
Br-2
Br-1
Tr-1
Tr-2
Br-1
Br-2
Tr-1
2 km
N
C
Tr-2
Tr-2
Tr-1
1 m
D
LI 43
LI 44
LI 51
Tr
(m)
Mud
Sand
Wavy-laminated heterolithic deposit
Lenticular heterolithic deposit
Cross-laminated or cross-stratified sand
Parallel-laminated sand
Massive sand
Massive mud
Laminated mud
Muddy peat
Pebble
Plant remain
Rootlet
Shell

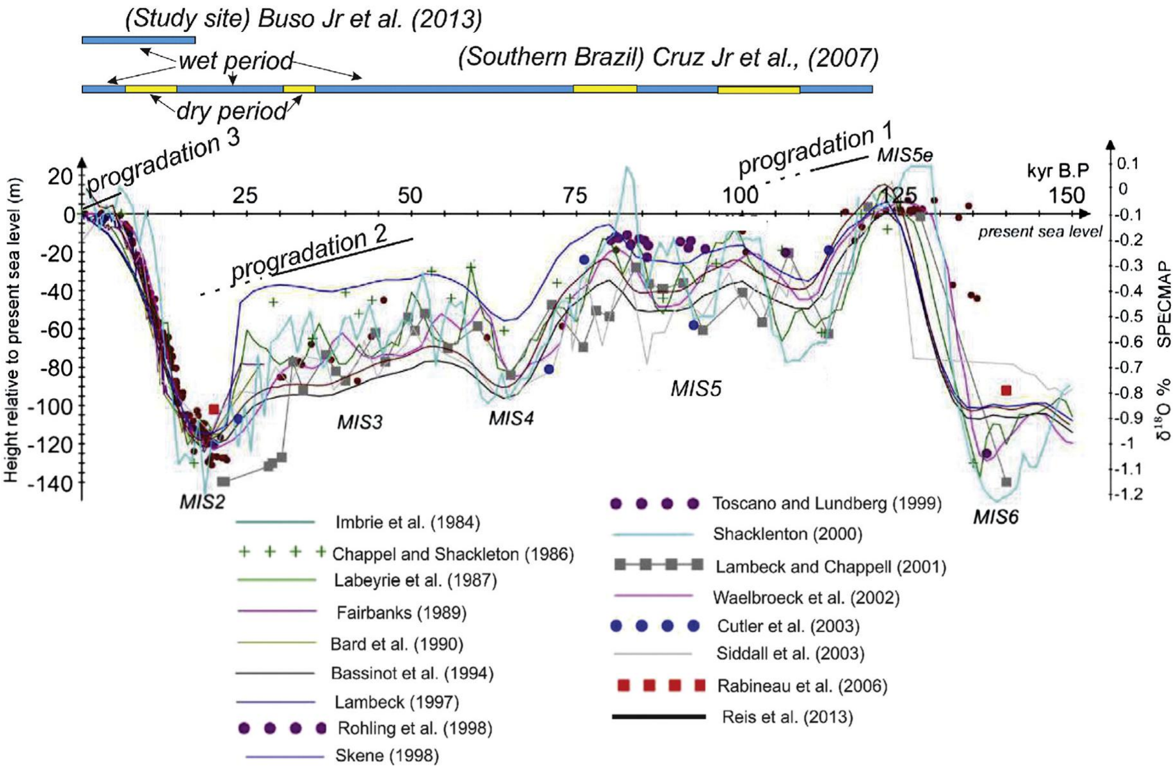


**Fig. 11.** Summary of the deltaic prograding events 1 to 3 in the study area within the context of sea-level changes proposed by previous publications for the study area and worldwide during the Late Pleistocene–Holocene (modified from Lambeck and Chappell, 2001; Reis *et al*., 2013).
Data from Bard et al. (1990), Bassinot et al. (1994), Chappell and Shackleton (1986), Imbrie (1984), Labeyrie et al. (1987), Lambeck (1997), Rohling et al. (1998), Siddall et al. (2003), Skene (1998) and Toscano and Lundberg (1999).

location closer to its modern course, but with the mouth circa 15 km northward of the present one (Fig. 12E). This process was accompanied by the development of a network of distributary channels along the delta plain.

The frequent changes in river dynamics over time produced significant channel scouring and mud deposition in interdistributary bays, which contributed to changing the nature of the delta in its central part. This process was responsible for the nearly complete destruction of beach ridges/spits of phase 2 in this central area (Figs. 2 and 12E), with the consequent preservation of only three discontinuous occurrences on these deposits on both sides of the modern Doce River. Concomitant to this process, the delta experienced renewed progradation, as recorded by beach ridges/spits of phase 3. This phase of delta progradation served to further define its cuspate geometry. The transportation of sand over great distances remains an ongoing process, as indicated by the occurrence of beach ridges under development 70 km northward of the modern river's mouth.

### *5.3. Sea-level history*

The evolution of the Doce River's delta presented here provides new insights into the history of relative sea-level changes on this coast since the Late Pleistocene. A recent study on this delta has evoked this issue (i.e., Cohen et al., 2014), but interpretations documented in that article were based on a restricted number of profiles along a single, 40 km-long, NNW–ESE trending transect located more than 50 km from the modern river's mouth. Our integration of geomorphological, sedimentological and chronological data provides a more comprehensive view of the various depositional environments, as well as of their spatial and temporal relationships. Consequently, the relative sea-level dynamics on this coast and their association with the Late Pleistocene–Holocene global sea-level history can be investigated in greater detail (Fig. 13).

The constraint of beach ridges/spits of phase 1 to the Barra Seca River, while the mouth of the Doce River underwent transgression, is compatible with local progradation along a coast with prevailing high sea level at 132,705 (±9152) ka, i.e., during the Last Interglacial (Fig. 13A, B). This period, also known as marine isotope stage (MIS) 5e or Eemian stage in Western Europe, started with a rapid warming at 130–140 ka (Stirling et al., 1995), which was followed by a global climate generally warmer and more humid than at present between 130 and 110 ka (see Adams et al., 1999 for a review). As a consequence, the global sea level was presumably 4 to 6 m (Veeh, 2012) or even 5.5 to 9 m (Dutton and Lambeck, 2012) higher than the present. A sea level as high as 8 to 10 m above the present level has been proposed for areas along the eastern and southern Brazilian coasts (Dominguez et al., 1981; Bittencourt et al., 1979; Martin et al., 1996).

The extensive delta progradation between 45,775–49,391 and 29,678–29,226 cal BP, recorded by beach ridges/spits of phase 2, occurred during the early stage of the Last Glaciation episode (Fig. 14C), which began ~60 ka ago. It has been suggested that temperatures dropped by up to 8 °C during this time (e.g., Ruddiman, 2008). This was accompanied by a progressive decrease in sea level (e.g., Crowley and North, 1991; Shackleton, 2000; Cutler et al., 2003; Rabineau et al., 2006), with estimates of nearly 120 m (Fairbanks, 1989; Clark et al., 2009), or at least 80 m (e.g., Cutler et al., 2003), below the modern sea level during the isotope stage 2 (MIS2) or LGM (23 and 18 ka) (e.g., Crowley and North, 1991). Thus, progradation of beach ridges/spits of phase 2 in the Doce River delta took place during a period of decreasing sea level that preceded the LGM.

**Fig. 10.** Transgressive deposits. A, B) PALSAR images with a RHH GHV BHH composition, illustrating the transgressive deposits of phases 1 (Tr-1) and 2 (Tr-2) and their spatial relationship with beach ridges/spits of phases 1 (Br-1) and 2 (Br-2). C) Field view of transgressive deposits of phase 1 (Tr-1) cut down by transgressive deposits of phase 2 (Tr-2). D) Lithostratigraphic profiles derived from core data representative of the vertical distribution of sedimentary facies. See Fig. 2 for location.

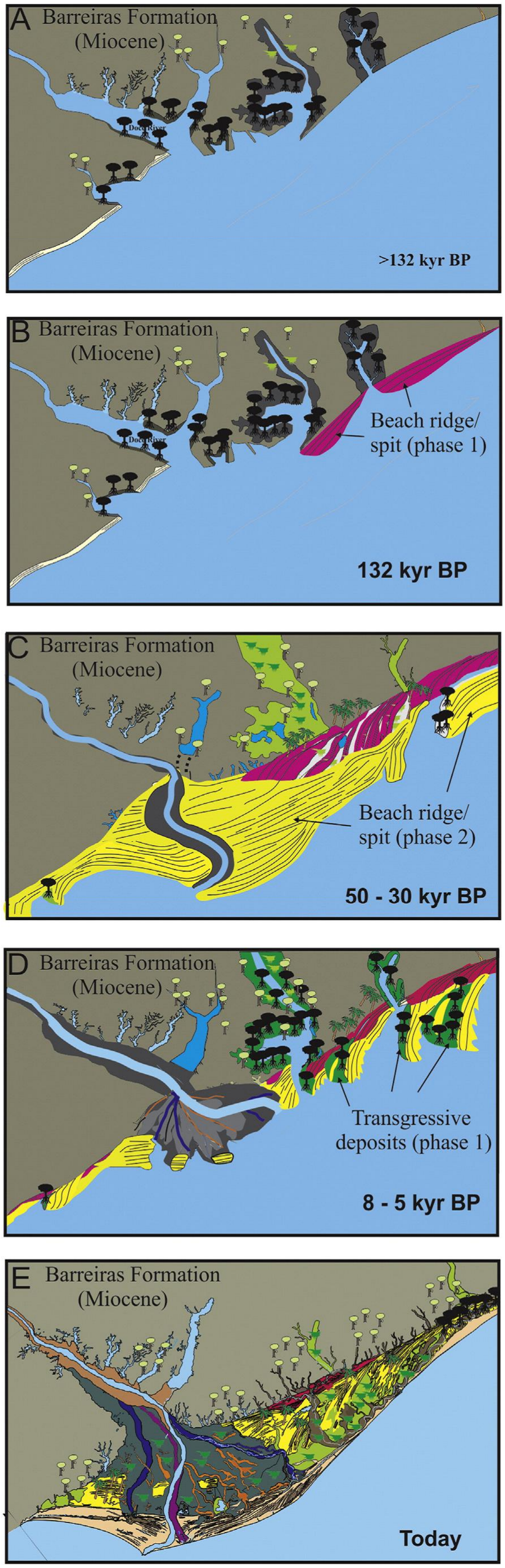


**Fig. 12.** A–E) Stages of morphological and sedimentary evolution proposed for the Doce River delta since the Miocene to the present time (see text for further explanations).

If the distance between the present and palaeo-shoreline at the delta front is of only 16 m (e.g., Polizel, 2014), and considering a change from the 8 m-highstand position in the previous interglaciation stage, then the beach ridges/spits of phase 2 would record a drop in relative sea level of less than 25 m. This is much lower than the global fall proposed for this period. In fact, a drop of several tens of meters as proposed would have caused coastal erosion instead of sediment deposition. Therefore, either the sea level was higher than proposed before the MIS 2 or the LGM, or the sea-level drop in the Doce River area was combined with other factors (e.g., tectonics) that would have compensated the sea level-fall. Alternatively, it is also possible to have a shelf delta formed by sediments that would have bypassed through the entire coastal system during this fall. In this case, the beach ridges/spits of phase 2 would represent a coastal delta progradation formed during the latest stage of progradation. These hypotheses are still open to debate, as it is the time when this phase of progradation ended. The young ages obtained from deposits located at the top of beach ridge/spits of phases 1 and 2 were interpreted as representative of reworked sands, probably as aeolian dunes.

The transgressive deposits of phase 1 indicate a relative sea-level high starting in the early Holocene (i.e., 8161–7933 cal yr BP) and continuing until the mid-Holocene (4974–4850 cal BP) (Fig. 13D). There has been no agreement about the global sea level in the Holocene. A rise by nearly 60 m has generally been accepted for most of the Earth between 11,650 and 7000 yr BP due to increased oceanic water volume following the LGM (see Smith et al., 2011 for a review). Despite this rise, a claim has been made that sea level was not higher than the present in the last 10 ka, as shown in some locations (e.g., Morhange et al., 2001). On the other hand, a worldwide rise of circa 5 m above the present has been proposed near the mid-Holocene (e.g., Crowley and North, 1991; Lambeck et al., 2002; Bard et al., 2010) (Fig. 13D). In many areas of the Brazilian coast (Martin and Suguio, 1992; Angulo et al., 2006; Rossetti et al., 2008; Reis et al., 2013) and of the South American coast (Milne et al., 2005), the sea level surpassed the present at 7000 yr BP (Suguio et al., 1985) by 4 to 6 m. The transgressive deposits of phase 1 could be taken as a further evidence of sea levels above the present level along the Brazilian coast near the early to mid-Holocene.

Although of limited extent, the delta formed when the Doce River occupied a northward position, as indicated by paleochannel 3, could suggest a relative sea-level drop of an uncertain age subsequent to the early to mid-Holocene transgression. High frequency relative sea-level oscillations during the late Holocene could have formed the transgressive deposits of phase 2, initiated at 4238–3455 yr BP (see Tables 2 and 3). Existing relative late Holocene sea-level curves during the last 5 ka for southeastern Brazil indicate either a continuous fall (Angulo et al., 2006) or a fall with punctuated rises between 4100–3800 and 3000–2700 yr BP (Suguio et al., 1985). The transgressive deposits of phase 2 could be a response to these sea-level changes or they could result from local oscillations in base level due to delta dynamics (Fig. 13E).

The beach ridges/spits of phase 3 record a renewed progradation as the Doce River shifted southward to occupy a position near to its modern course (Fig. 13E). The age of these deposits remains to be determined, but the presence of these prograding beach ridges/spits in the late Holocene is in agreement with the overall drop in sea level recorded in the southeastern and northeastern Brazilian littoral (Angulo et al., 2006). Hence, such an event may have accompanied the global trend of falling sea level after the early to mid-Holocene transgression.

### 5.4. *Influence of climate*

The early to mid-Holocene transgression has not significantly affected the central delta area, which continued being dominated by fluvial

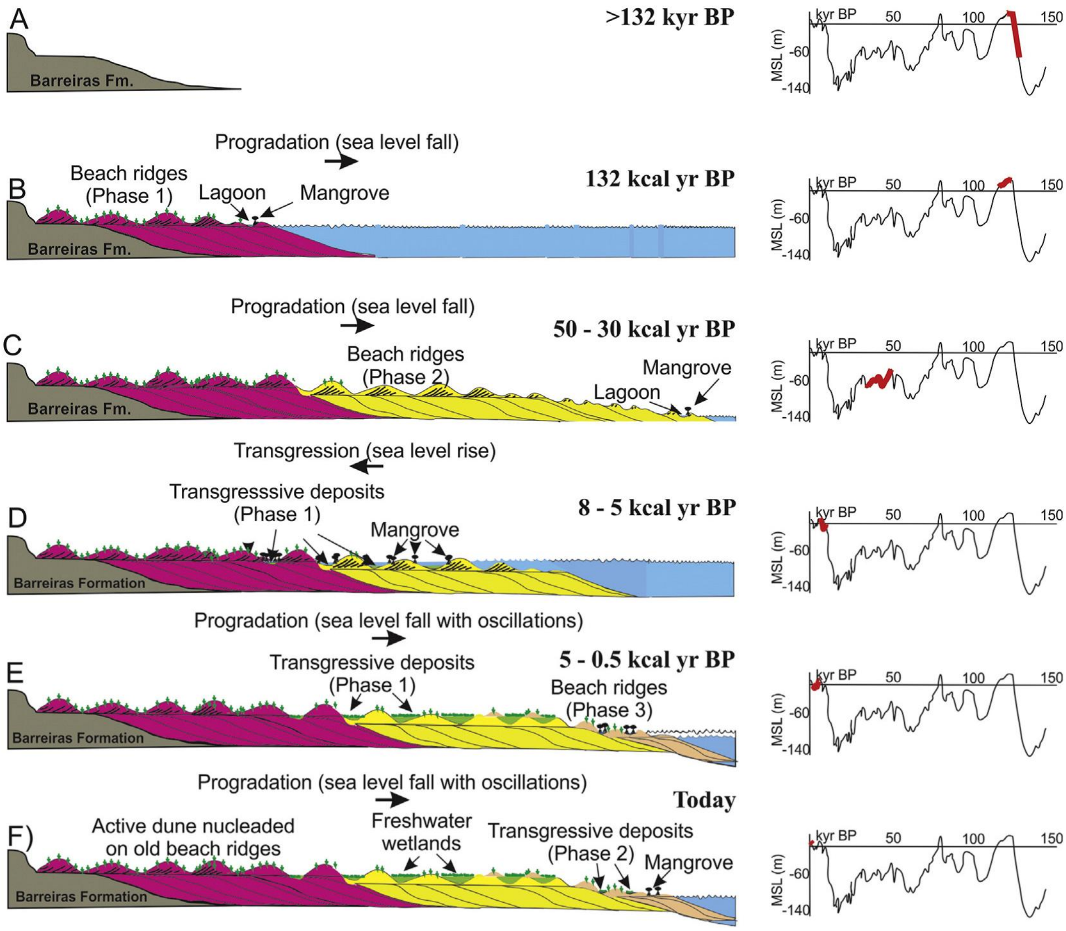


**Fig. 13.** A–F) Proposed sedimentary evolution of the Doce River delta within the context of sea- level changes (sea-level curves depicted in the right diagrams from Waelbroeck et al., 2002; see text for further explanations).

processes. It follows that it is difficult to relate delta dynamics merely to relative sea-level changes. The ongoing development of the Doce River delta during the post-glacial sea-level rise may be explained by the balance between sediment supplied to the coastal system and relative sea level. When sufficient sediment enters into a coastal system to equalize the amount of space available, the previous coastal system is kept stable independently of sea level rises (Posamentier et al., 1992).

Studies have inferred a relatively dry period in southeastern Brazil for the early and mid-Holocene (e.g., Behling et al., 2004; Pessenda et al., 2004; Cruz et al., 2007). However, publications based on palynology have inferred a humid climate in the Atlantic forest during the entire Holocene (e.g., Behling and Negrelle, 2001). Additionally, recent pollen and isotope works carried out on the northern coast of the State of Espírito Santo near the study area suggested a relatively humid climate from ~17,000 cal yr BP, with increased humidity between ~7000 and 4000 cal yr BP (Buso et al., 2013) (Fig. 11). Thus, despite the post-glacial sea-level rise, the higher rainfall associated with the humid climate recorded over the drainage basin of the Doce River during the Holocene probably allowed the studied deltaic system to keep pace with the relative sea-level rise, at least in the central delta exposed to stronger influence of the Doce River.

### 5.5. The wave-influenced delta model

The existing investigation supporting that numerous factors may affect the evolution of deltaic depositional systems has precluded the establishment of a single facies model, and even has us led to conclude that each delta system may be in reality unique (Elliot, 2014). Despite this complexity, a tripartite model that takes into account the interplay of wave, tide and fluvial flows has been widely used, as these processes are of primary relevance to define deltaic morphologies and facies stratal patterns (e.g., Galloway, 1975). Among the delta types defined by this model, wave-influenced deltas are highly complex because they can contain numerous depositional environments, such as lagoons, estuaries and marshes, which are also common to other coastal settings. This fact may represent a problem for interpreting past deltaic sedimentary successions.

Bhattacharya and Giosan (2003) predicted facies distribution applying the asymmetry index to express the degree of dominance of marine versus fluvial processes for a series of wave-influenced deltas. In general, increasing facies asymmetry occurs with stronger longshore drift caused by consistent wave dislocation in one direction. Hence, symmetrical deltas generally have straight and gently curved beach ridges equally distributed on both sides of river mouths, while asymmetrical and deflected deltas, which have increasingly stronger net sediment distribution, would present thicker beach ridge sandy bodies and muddier deposits in the updrift and downdrift sides of the river mouths, respectively.

As previously discussed in this work, the Doce River delta displays a cuspate geometry that is typical of wave-influenced deltas. The wave-dominated model based on the asymmetrical index, however, may be not applicable. Indeed, the most extensive beach ridge/spit deposits of phase 2 were formed on both sides of the river mouths. The southern paleochannel responsible for sediment influx during this time was, however, deflected southward and then northward (see Fig. 2), presumably due to changes in longshore current. In addition, most of the beach ridge/spit deposits of phase 3 were formed while the Doce River occupied a northward position with respect to its modern course

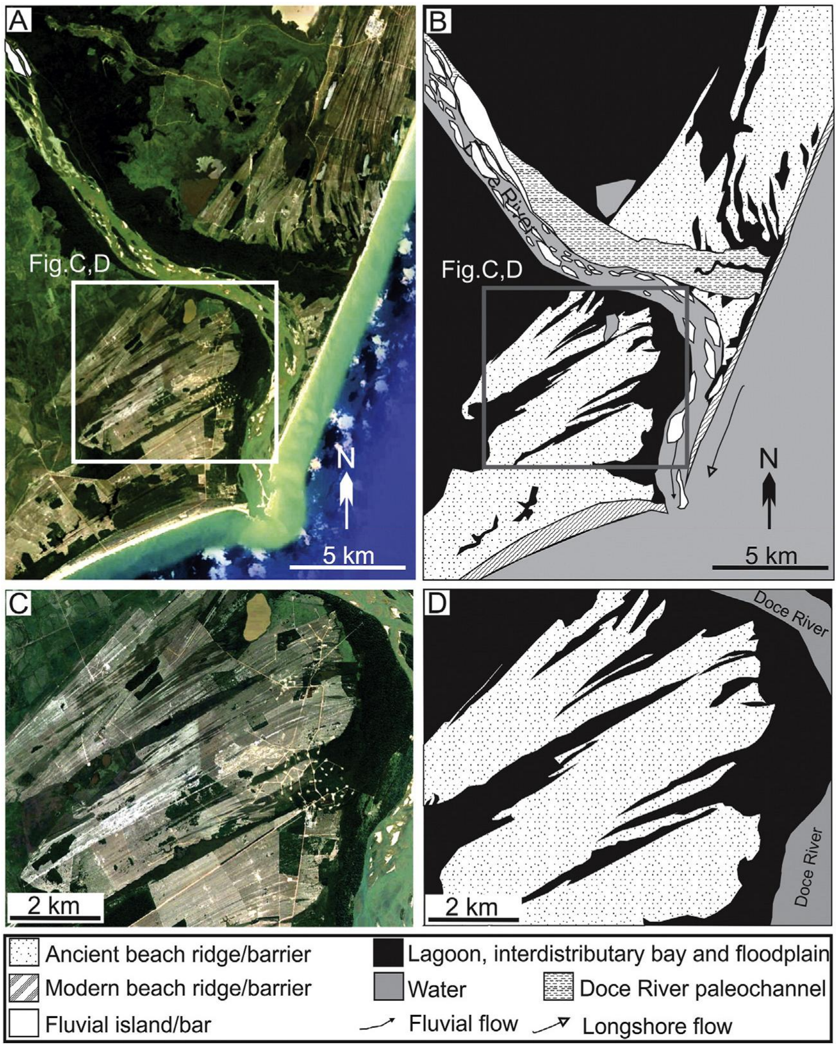


**Fig. 14.** Distribution of sedimentary deposits of beach ridges/spits of phase 3 in the Doce River delta. A, B) Google Image (A) and corresponding line drawing (B) illustrating a close up the river's mouth, which was deflected northward in the past and then southward in the recent time. Note that the beach ridge/spit deposits are fairly equally distributed on both sides of the river. C, D) Detail of figures A and B, illustrating the prevalence of beach ridge/spit deposits subordinately alternated a few muddy deltaic deposits, a pattern also observed northward of this river's mouth.

(Figs. 2 and 14). Despite the terminal segment of this paleochannel having a deflection suggestive of a northward longshore drift, the beach ridge/spit sand bodies have equivalent proportions of environments prone to mud deposition, such as lagoons, and they are equally distributed on the updrift and downdrift sides of its mouth (Fig. 14A, B). In addition, the modern channel, which is currently located southward of this paleochannel, was strongly deflected southward. However, as opposed to prediction by the asymmetrical index model of wave-influenced deltas, a continuous sandy body was deposited in the downdrift side of the modern river mouth, while a barrier island with an associated lagoon where mud deposition takes place is currently present updrift of this mouth. A previous publication has also indicated inconsistencies of the asymmetry index of wave-influenced deltas (Anthony, 2015).

An analysis of other wave-influenced deltas of the Brazilian coast leads us to conclude that the Doce River delta is not the only exception not conforming to the asymmetrical wave-dominated delta model of Bhattacharya and Giosan (2003). For instance, the Peixoto River delta in Caravelas, State of Bahia (e.g., Martin et al., 1980; Martin and Dominguez, 1994) was strongly deflected northward by a northward longshore current (Fig. 15A–B). Despite this fact, the sandy beach ridges are all concentrated in the downdrift side of this river's mouth, while its updrift side is dominated by low energy, muddy-prone environments. Northward, the São Francisco delta at the border of the States of Alagoas and Sergipe, which is used as the classical example of wave-dominated deltas (e.g., Galloway, 1975), had a stable course through the delta evolution resulting from a strong northward, and then southward deflection of its mouth through time (Fig. 15C–D). Despite this pattern, there is a fairly equal proportion of sandy beach ridges when both margins of this river are compared. The apparent amalgamated beach ridges located in the delta's northward side in fact alternate with numerous narrow lagoon environments (Fig. 15E–F) similar to the beach ridges of the delta's southward margin. Furthermore, despite the fact that the mouth of this river has been deflected southward more recently, its downdrift side developed a lagoon–barrier island system. In contrast, windblown sand sheets, probably representative of reworked beach ridges, prevail in the updrift side of this river's mouth, a process also active southward of the lagoon–barrier island system formed southward (Fig. 15D). Likewise, the Jequitinhonha delta in southern Bahia (e.g., Bittencourt et al., 2011) appears to have been strongly deflected southward in the past, although beach ridge deposits are present on both margins of the main river, even with a higher proportion in the downdrift side of this river's mouth. Only more recently has the northward deflection of the river's mouth favored the development of a barrier island system in its downdrift side, while beach ridges were formed updrift of the river's mouth.

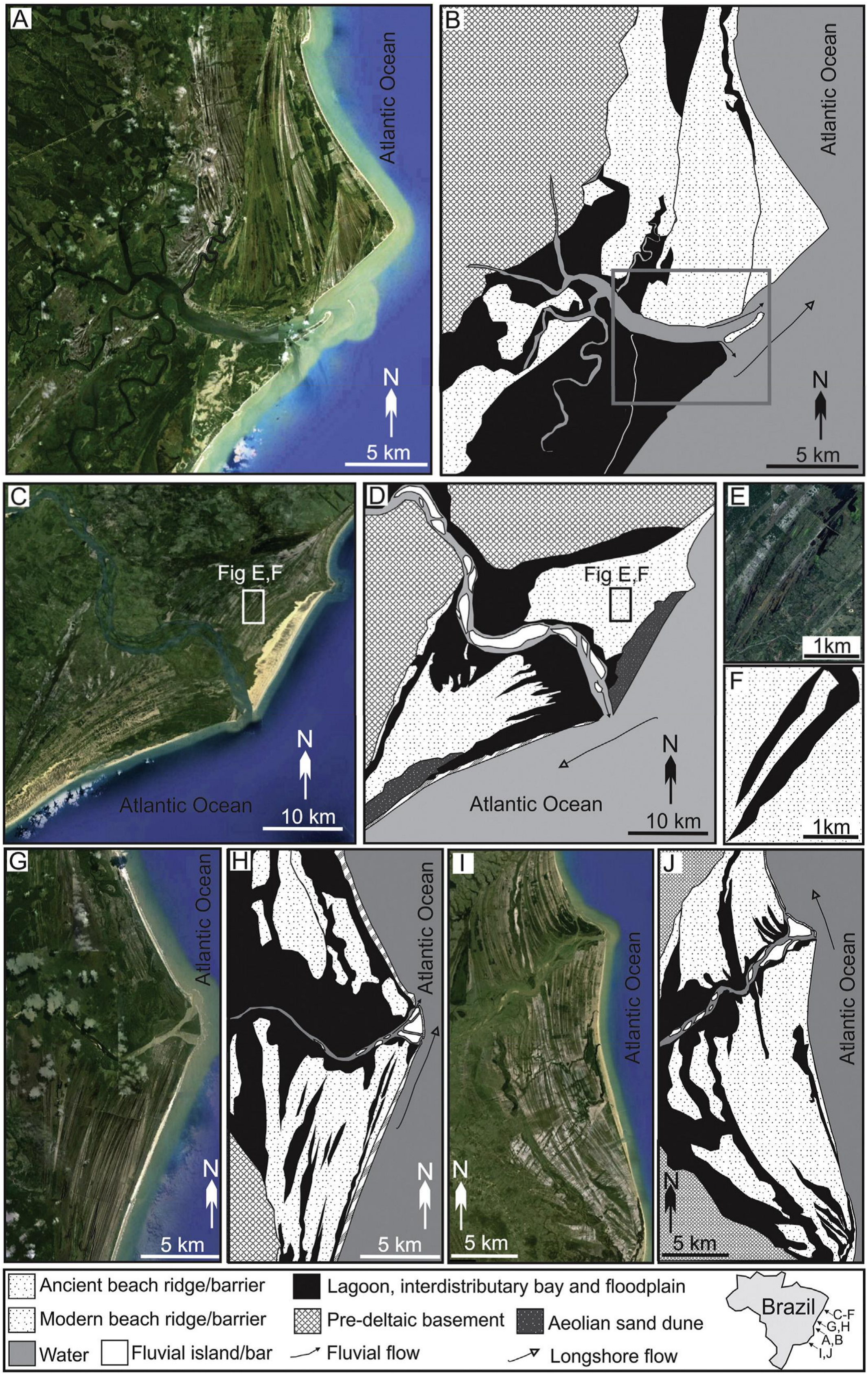


**Fig. 15.** Examples of wave-influenced deltas along the northeastern coast of Brazil. A, B) Peixoto River delta. C–F) São Francisco delta. G, H) Jequitinhonha delta. I, J) Paraíba do Sul delta (see text for explanations).

The Paraíba do Sul delta, located in the northern part of the State of Rio de Janeiro (Fig. 15I, J), displays a fairly symmetrical facies distribution, with sides of the river's mouth been dominated by beach ridge deposits subordinately alternated with a few narrow and elongated muddy lagoon deposits, despite the progressive overall northward deflection of the river course through time.

The lack of agreement in terms of facies distribution observed between the asymmetry index deltaic model and several wave-dominated deltas from the Brazilian coast, as discussed here and also previously presented by Anthony (2015), conforms to the proposal that other factors than only the simple interplay of riverine versus marine processes influence the evolution of a delta and the changes in its morphology over time. Sea-level fluctuation has been suggested as an important factor to have influenced the evolution of the Brazilian deltas (e.g., Dominguez, 1996). However, a recent publication (i.e., Lima et al., 2014) showed that the morphology and sedimentary deposition of the São Francisco delta were controlled by N–S to NE–SW trending normal faults reactivated in the Quaternary, which might have also been the instance of many other areas of the Brazilian margin (see also Nogueira et al., 2010; Bezerra et al., 2014; Rossetti et al., 2011, 2013). Previous publications (e.g., Hatushika et al., 2007; Bricalli and Mello, 2013) have also suggested that the evolution of the Doce River delta was controlled by tectonic activity contemporaneous to sediment deposition. However, as shown in the present work, sea-level change constituted an important element in determining facies distribution in the Doce River delta. Therefore, additional investigations are still required in order to further demonstrate the factor of primordial influence in the distribution of facies patterns in this and in other wave-influenced deltas of the Brazil's coast.

## 6. Conclusions

This survey led to conclude that the Doce River delta was formed by sand progradation directly into an open marine environment since its earliest development in the Late Pleistocene, instead of having an initial lagoonal phase only in the mid-Holocene as previously proposed. Despite the wave-influenced nature, this delta had an important contribution of fluvial sediments, which were reworked by wave-generated longshore transport to form a series of beach ridges/spits on both sides of the main river. The several positions occupied by the Doce River along the delta plain during its evolution and the transgressive episodes mainly between 8161–7933 and 4974–4850 cal yr BP resulted in significant erosion of deltaic deposits formed during two phases of main progradation, i.e., at 132,705 (±9152) ka and between 29,678–29,226 and 45,775–49,391 cal yr BP, the latter corresponding to the Last Glaciation sea-level drop. The Doce River delta started to grow again with the global trend of falling sea-level after the late-Holocene transgression, a process which is ongoing at the present time. Analysis of this delta and its comparison with several other wave-influenced deltas of the Brazil's coast reveals that they do not present facies distributions compatible to the pattern predicted by current wave-influenced delta models. The expected increased proportion of sandy- and muddy-prone deposits in the updrift and downdrift sides of a deflected river's mouth, respectively, is not applicable. The evolution of the wave-influenced Brazilian deltas seems to be much more complex due to other controlling factors than simply the interplay of fluvial and marine processes predicted by asymmetry index models. Hence, sea-level fluctuations and tectonic reactivations, and possibly also changes in sediment discharge due to climatic influences, must be better investigated as important determinants of the morphology and facies stratal patterns in these deltas. More detailed studies of these deltas can contribute to improve available wave-influenced delta models, and particularly to apply process-based facies models to reconstruct these systems in the sedimentary record.

## Acknowledgments

This work was financed by FAPESP (Project # 2007/03615-5, 2011/00995-7 and 2009/53988-8). All authors hold fellowships from CAPES and CNPq. The Vale Natural Reserve in Linhares, State of Espírito Santo, and the Brazilian Institute for Space Research—INPE provided logistical support for fieldwork. Dr. André O. Sawakushi and M.Sc. Edipo Henrique Cremon are acknowledged for helping with the OSL analyses. Dr. Edward Anthony, Dr. Brian Willis, one anonymous reviewer and the Editor-in-chief Dr. John T. Wells made several suggestions and corrections that contributed to improve an early version of the manuscript.

## References

Adams, J., Maslin, M., Thomas, E., 1999. Sudden climate transitions during the Quaternary. Prog. Phys. Geogr. 23, 11–36.
Angulo, R.J., Lessa, G.C., Souza, M.C., 2006. A critical review of mid- to late-Holocene sea-level fluctuations on the eastern Brazilian coastline. Quat. Sci. Rev. 25, 486–506.
Anthony, E., 2015. Wave influence in the construction, shaping and destruction of river deltas: a review. Mar. Geol. 361, 53–78.
Bacoccoli, G., 1971. Os deltas marinhos holocênicos brasileiros: uma tentativa de classificação. Bol. Técnico Petrobrás 14, 5–38.
Bandeira Jr., A.N., Petri, S., Suguio, K., 1975. Projeto Rio Doce (Final report). Petrobrás-CENPES, Rio de Janeiro, Brazil (203 pp.).
Bard, E., Hamelin, B., Delanghe-Sabatier, D., 2010. Deglacial meltwater pulse 1B and Younger Dryas sea levels revisited with boreholes at Tahiti (and supporting online material). Science 327, 241–244.
Bard, E., Hamelin, B., Fairbanks, R.G., 1990. U-Th ages obtained by mass spectrometry in corals from Barbados: sea level during the past 130,000 years. Nature 346, 456–458.
Bassinot, F.C., Labeyrie, L.D., Vincent, E., Quidelleur, X., Shackleton, N.J., Lancelot, Y., 1994. The astronomical theory of climate and the age of the Brunhes-Matuyama magnetic reversal. Earth and Planet. Sci. Lett. 126, 91–108.
Behling, H., Negrelle, R.R.B., 2001. Tropical rain forest and climate dynamics of the Atlantic Lowland, Southern Brazil, during the Late Quaternary. Quat. Res. 56, 383–389.
Behling, H., Cohen, M.C.L., Lara, R.J., 2004. Late Holocene mangrove dynamics of the Marajó Island in northern Brazil. Veg. Hist. Archaeobot. 13, 73–80.
Bezerra, F.H.R., Rossetti, D.F., Oliveira, R.G., Medeiros, W.E., Neves, B.B.B., Balsamo, F., Nogueira, F.C.C., Dantas, E.L., Andrades Filho, C., Góes, A.M., 2014. Neotectonic reactivation of shear zones and implications for faulting style and geometry in the continental margin of NE Brazil. Tectonophysics 614, 78–90.
Bhattacharya, J.P., Giosan, L., 2003. Wave-influenced deltas: geomorphological implications for facies reconstruction. Sedimentology 50, 187–210.
Bittencourt, A.C.S.P., Martin, L., Vilas-Boas, G.S., Flexor, J.M., 1979. The marine formations of the coast of the State of Bahia (Brazil). In: Suguio, K., Fairchild, R.R., Martin, L., Flexor, J.-M. (Eds.), Proceedings of the 1978 International Symposium on Coastal Evolution in the Quaternary, São Paulo, pp. 232–253.
Bittencourt, A.C.S.P., Dominguez, J.M.L., Martin, L., Silva, I.R., Medeiros, K.O.P., 2007. Past and current sediment dispersion pattern estimates through numerical modeling of wave climate: an example of the Holocene delta of the Doce River, Espírito Santo, Brazil. An. Acad. Bras. Cienc. 79, 333–341.
Bittencourt, A.C.S.P., Dominguez, J.M.L., Tanajura, C.A.S., Silva, I.R., Martin, L., 2011. A diachronic view of the net longshore sediment drift during the late Holocene at the Jequitinhonha River delta, Brazil, using numerical modelling. An. Acad. Bras. Cienc. 83, 1207–1219.
Bricalli, L.L., Mello, C.L., 2013. Padrões de lineamentos relacionados a litoestrutura e fraturamento neotectônico (Estado do Espírito Santo, SE do Brasil). Rev. Bras. Geogr. 14, 301–311.
Buso Jr., A.A., Pessenda, L.C.R., Oliveira, P.E., Giannini, P.C.F., Cohen, M.C.L., Volkmer-Ribeiro, C., Oliveira, S.M.B., Favaro, D.I.T., Rossetti, D.F., Lorente, F.L., Borotti Filho, M.A., Schiavo, J.A., Bendassolli, J.A., Franca, M.C., Guimaraes, J.T.F., Siqueira, G.S., 2013. From an estuary to a freshwater lake: a paleo-estuary evolution in the context of Holocene sea-level fluctuations, southeastern Brazil. Radiocarbon 55, 1735–1746.
Castro, D.F., Rossetti, D.F., Cohen, M.C.L., Pessenda, L.C.R., Lorente, F.L., 2013. The growth of the Doce River Delta in northeastern Brazil indicated by sedimentary facies and diatoms. Diatom Res. 28, 455–466.
Chappell, J., Shackleton, N.J., 1986. Oxygen isotopes and sea level. Nature 324, 137–140.
Clark, P.U., Dyke, A.S., Shakun, J.D., Carlson, A.E., Clark, J., Wohlfarth, B., Mitrovica, J.X., Hostetler, S.W., McCabe, M., 2009. The Last Glacial Maximum. Science 325, 710–714.
Coelho, A.L.N.C., 2007. Alterações hidrogeomorfologia do médio-baixo Rio Doce (Doctoral Thesis). Universidade Estadual Fluminense, Niterói, Rio de Janeiro.
Cohen, M.C.L., França, M.C., Rossetti, D.F., Pessenda, L.C.R., Giannini, P.C.F., Lorente, F.L., Buso Jr., A.A., Castro, D., Macario, K., 2014. Landscape evolution during the late Quaternary at the Doce River mouth, Espírito Santo State, Southeastern Brazil. Palaeogeogr. Palaeoclimatol. Palaeoecol. 415, 48–58.
Coleman, J.M., Wright, L.D., 1975. Modern river deltas: variability of processes and sand bodies. In: Broussard, M.L. (Ed.), Deltas, Models for Exploration. Houston Geological Society, Houston, TX, pp. 99–149.
Crowley, T.J., North, G.R., 1991. Paleoclimatology. Oxford University Press, Oxford (339 pp.).
Cruz Jr., F.W., Burns, S.J., Jercinovic, M., Karmann, I., Sharp, W.D., Vuille, M., 2007. Evidence of rainfall variations in Southern Brazil from trace element ratios (Mg/Ca and Sr/Ca) in a Late Pleistocene stalagmite. Geochim. Cosmochim. Acta 71, 2250–2263.

Cutler, K.B., Edwards, R.L., Taylor, F.W., Cheng, H., Adkins, J., Gallup, C.D., Cutler, P.M., Burr, G.S., Bloom, A.L., 2003. Rapid sea-level fall and deep ocean temperature change since the last interglacial period. Earth Planet. Sci. Lett. 206, 253–271.
Dominguez, J.M.L., 1996. The São Francisco strandplain: a paradigm for wave-dominated deltas? In: De Baptist, M., Jacobs, P. (Eds.), Geology of siliciclastic shelf seas 117. Special Publication of the Geological Society of London, pp. 217–231
Dominguez, J.M.L., Bittencourt, A.C.S.P., Martin, L., 1981. Esquema evolutivo da sedimentação quaternária nas feições deltáicas do rio São Francisco (SE/AL), Jequitinhonha (BA), Doce (ES) e Paraíba do Sul (RJ). Rev. Bras. Geosci. 11, 227–237.
Dominguez, J.M.L., Bittencourt, A.C.S.P., Martin, L., 1983. Papel da deriva litorânea de sedimentos arenosos na construção das planícies costeiras associadas às desembocaduras dos rios São Francisco (SE-AL), Jequitinhonha (BA) e Paraíba do Sul (RJ). Rev. Bras. Geosci. 13, 98–105.
Dominguez, J.M.L., Bittencourt, A.C.S.P., Martin, L., 1987. Sea-level history and Quaternary evolution of river mouth-associated beach-ridge plains along the east-southeast Brazilian coast: a summary. In: Nummedal, D., Pilkey, O.H., Howards, J.D. (Eds.), Sea-level Fluctuation and Coastal Evolution. Special Publication of the Society of Economic Paleontologists and Mineralogists 41, pp. 115–127.
Dutton, A., Lambeck, K., 2012. Ice volume and sea level during the Last Interglacial Science 337. pp. 216–219.
Elliot, T., 2014. Deltaic systems and their contribution to an understanding of basin-fill successions. Geol. Soc. Lond. Spec. Publ. 1989, 3–10.
Fairbanks, R.G., 1989. A 17,000-year glacio-eustatic sea level record: Influence of glacial melting rates on the Younger Dryas event and deep-ocean circulation. Nature 342, 637–642.
França, R.L., Del Rey, A.C., Tagliari, C.V., Brandão, J.R., Fontanelli, P.R., 2007. Bacia do Espírito Santo. Bol. Geociências Petrobrás 15, 501–509.
França, M.C., Cohen, M.C.L., Pessenda, L.C.R., Rossetti, D.F., Lorente, F.L., Buso Jr., A.A., Guimarães, J.T.F., Friaes, Y., 2013. Mangrove dynamics in response to sea-level changes on Holocene terraces of the Doce River, southeastern Brazil. Catena 110, 59–69.
Galloway, W.E., 1975. Process framework for describing the morphologic and stratigraphic evolution of deltaic depositions systems. In: Broussard, M.L. (Ed.), Deltas, Models of Exploration, pp. 87–98.
Galloway, W.E., Hobday, D.K., 1996. Terrigenous Clastic Depositional Systems. Springer-Verlag, Heidelberg (489 pp.).
Goudie, A.S., 2004. Encyclopedia of Geomorphology. International Association of Geomorphologists. v. 1. Taylor & Francis Group (1202 pp.).
Hatushika, R.S., Silva, C.G., Mello, C.L., 2007. Sismoestratigrafia de alta resolução no lago Juparanã, Linhares (ES-Brasil) como base para estudos sobre a sedimentação e tectônica quaternária. Rev. Bras. Geofis. 25, 433–442.
IBGE—Instituto Brasileiro de Geografia e Estatística, 1987. Carta do Brasil. Folha SE-24 Rio Doce: geologia, geomorfologia, pedologia, vegetação, uso potencial da terra, Rio de Janeiro (548 pp.).
Imbrie, J., Hays, J.D., Martinson, D.G., McIntyre, A., Mix, A.C., Morley, J.J., Pisias, N.G., Prell, W.L., Shackleton, N.J., 1984. The orbital theory of Pleistocene lcimate: support from a revised chronology of the marine 18O record. In: Berger, A., Imbrie, J., Hays, J., Kukla, G., Saltzman, B. (Eds.), Milankovich and Climate. Reidel, Dordrecht, pp. 269–306.
INPE—Instituto Nacional de Pesquisas Espaciais, 2013. Catálogo de imagens. Available at, http://www.dgi.inpe.br/CDSR/ (Access in October 10th, 2013).
Köppen, W., 1948. Climatologia: con un Estudio de los Llimas de la Tierra. Fondo de Cultura Econômica, México, D.F. (479 pp.).
Labeyrie, L.D., Duplessy, J.C., Blanc, P.L., 1987. Variations in mode of formation and temperature of oceanic deep waters over the past 125,000 years. Nature 327, 477–482.
Lambeck, K., 1997. Sea-level change along the French Atlantic and Channel coasts since the time of the Last Glacial Maximum. Palaeogeogr. Palaeoclimatol. Palaeoecol. 129, 1–22.
Lambeck, K., Chappell, J., 2001. Sea level change through the last glacial cycle. Science 292, 679–686.
Lambeck, K., Yokoyama, Y., Purcell, T., 2002. Into and out of the Last Glacial Maximum: sea-level change during oxygen isotope stages 3 and 2. Quat. Sci. Rev. 21, 343–360.
Lima, C.C.U., Bezerra, F.H.R., Nogueira, F.C., Maia, R.P., Sousa, M.O.L., 2014. Quaternary fault control on the coastal sedimentation and morphology of the São Francisco coastal plain, Brazil. Tectonophysics 633, 98–114.
Martin, L., Dominguez, J.M.L., 1994. Geological history of coastal lagoons. In: Kjerfve, B. (Ed.), Coastal Lagoon Processes. Oceanography Series 60. Elsevier, pp. 41–68.
Martin, L., Suguio, K., 1992. Variation of coastal dynamics during the last 7000 years recorded in beach-ridge plains associated with River mouths: example from the central Brazilian coast. Palaeogeogr. Palaeoclimatol. Palaeoecol. 99, 119–140.
Martin, L. Bittencourt, A.C.S.P., Vilas Boas, G.S., Flexor, J.M., 1980. Mapa geológico do Quaternário costeiro do Estado da Bahia, escla 1:250,000. Secretaria de Minas e Energia, Governo do Estado da Bahia, Brazil.
Martin, L., Suguio, K., Flexor, J.-M., 1993. As flutuações do nível do mar durante o Quaternário superior e a evolução geológica de "deltas" brasileiros. Boletim de Geologia do Instituto de Geociências/USP 15, pp. 1–186.
Martin, L., Suguio, K., 1987. Quaternary evolution of the central part of the Brazilian coast: the role of relative sea-level variation and of shoreline drift. Quaternary coastal geology of West Africa and South America 43. United Nations Educational, Scientific and Cultural Organization Reports in Marine Science, pp. 97–145.
Martin, L., Suguio, K., Flexor, J.-M., Dominguez, J.M., Bittencourt, A.C.S.P., 1996. Quaternary sea-level history and variation in dynamics along the central Brazilian coast: consequences on coastal plain construction. An. Acad. Bras. Cienc. 68, 303–354.
Martin, L., Dominguez, J.M.L., Bittencourt, A.C.S.P., 2003. Fluctuating Holocene sea levels is eastern and southeastern Brazil: evidence from a multiple fossil and geometric indicators. J. Coast. Res. 19, 101–124.
Millani, E.J., Brandão, J.A.S.L., Zalán, P.V., Gamboa, L.A.P., 2001. Petróleo na margem continental brasileira: geologia, exploração, resultados e perspectivas. Braz. J. Geophys. 18, 351–396.
Milne, G.A., Long, A.J., Bassett, S.E., 2005. Modelling Holocene relative sea-level observations from the Caribbean and South America. Quat. Sci. Rev. 24, 1183–1202.
Morhange, C., Laborel, J., Hesnard, A., 2001. Changes of relative sea level during the past 5000 years in the ancient harbor of Marseilles, Southern France. Palaeogeogr. Palaeoclimatol. Palaeoecol. 166, 319–329.
Murray, A.S., Wintle, A.G., 2003. The single Aliquot regenerative dose protocol: potential for improvements in reliability. Radiat. Meas. 37, 377–381.
Nogueira, F.C., Bezerra, F.H.R., Fuck, R.A., 2010. Quaternary fault kinematics and chronology in intraplate northeastern Brazil. J. Geodyn. 49, 79–91.
Pessenda, L.C.R., Ribeiro, A.S., Gouveia, S.E.M., Aravena, R., Boulet, R., Bendassoli, J.A., 2004. Vegetation dynamics during the late Pleistocene in the Barreirinhas region, Maranhão State, northeastern Brazil, based on carbon isotopes in soil organic matter. Quat. Res. 62, 183–193.
Polizel, S.P., 2014. Caracterização morfológica do delta do rio Doce (ES) com base em sensoriamento remoto (M.Sc. Thesis), Instituto Nacional de Pesquisas Espaciais—INPE, São José dos Campos, SP (130 pp.).
Polizel, S.P., Rossetti, D.F., 2014. Caracterização morfológica do delta do rio Doce (ES) com base em análise multissensor. Rev. Bras. Geogr. 15, 311–326.
Posamentier, H.W., Allen, G.P., James, D.P., Tesson, M., 1992. Forced regressions in a sequence stratigraphic framework: concepts, examples, and exploration significance. Am. Assoc. Pet. Geol. Bull. 76, 1687–1709.
Prescott, J.R., Stephan, L.G., 1982. The contribution of cosmic radiation to the environmental dose for thermoluminescence dating. Proceedings of the Second Specialist Seminar on Thermoluminescence Dating 6. Council of Europe, Strasbourg, pp. 17–25.
Rabineau, M., Berné, S., Aslanian, D., Olivet, J.L., Joseph, P., Guillocheau, F., Bourillet, J.F., Ledrezen, E., Granjeon, D., 2006. Paleo sea levels reconsidered from direct observation of paleoshoreline position during Glacial Maxima (for the last 500,000 yr). Earth Planet. Sci. Lett. 252, 119–137.
Reimer, P.J., Baillie, M.G.L., Bard, E., Bauliss, A., Beck, J.W., Blackwell, P.G., Ramsey, C.B., Buck, C.E., Burr, G.S., Edwards, R.L., Friedrich, M., Grootes, P.M., Guilderson, T.P., Hajdas, I., Heaton, T.J., Hogg, A.G., Hughen, K.A., Kaiser, K.F., Kromer, B., McCormac, F.G., Manning, S.W., Reimer, R.W., Richards, D.A., Southon, J.R., Tálamo, S., Turney, C.S.M., Van Der Licht, J., Weyhenmeyer, C.E., 2009. IntCal09 and Marine09 radiocarbon age calibration curves, 0–50,000 years cal BP. Radiocarbon 51, 1111–1150.
Reis, A.T., Maia, R.M.C., Silva, C.G., Rabineau, M., Guerra, J.V., Gorini, C., Ayres, A., Oliveira, R.A., Benabdellouahed, M., Simões, I.C.V.P., Tardin, R., 2013. Origin of step-like and lobate seafloor features along the continental shelf off Rio de Janeiro State, Santos basin—Brazil. Geomorphology 203, 25–45.
Rohling, E.J., Fenton, M., Jorissen, F.J., Bertrand, P., Ganssen, G., Caulet, J.P., 1998. Magnitudes of sea-level lowstands of the past 500,000 years. Nature 394, 162–165.
Rossetti, D.F., Valeriano, M.M., Góes, A.M., Thalles, M., 2008. Palaeodrainage on Marajó Island, northern Brazil, in relation to Holocene relative sea-level dynamics. The Holocene 18, 1–12.
Rossetti, D.F., Bezerra, F.H.R., Góes, A.M., Neves, B.B.B., 2011. Sediment deformation in Miocene and post-Miocene strata, Northeastern Brazil: evidence for paleoseismicity in a passive margin. Sediment. Geol. 235, 172–187.
Rossetti, D.F., Bezerra, F.H.R., Dominguez, J.M.L., 2013. Late Oligocene–Miocene transgressions along the equatorial and eastern margins of Brazil. Earth Sci. Rev. 123, 87–112.
Ruddiman, W.F., 2008. Earth's Climate—Past and Future. W.H. Freeman and Company, New York (388 pp.).
Shackleton, N.J., 2000. The 100,000-year Ice-Age cycle identified and found to lag temperature, carbon dioxide, and orbital eccentricity. Science 289, 1897–1902.
Siddall, M., Rohling, E.J., Almogi-Labin, A., Hemleben, C., Meischner, D., Schmelzer, I., Smeed, D.A., 2003. Sea-level fluctuations during the last glacial cycle. Nature 423, 853–858.
Skene, K.I., 1998. Evaluation of the global oxygen isotope curve as a proxy for Quaternary sea level by modeling of delta progradation. J. Sed. Res. 68, 1077–1092.
Smith, D.E., Harrison, S., Firth, C.R., Jordan, J.T., 2011. The early Holocene sea level rise. Quat. Sci. Rev. 30, 1846–1860.
Stirling, C.H., Esat, T.M., McCulloch, M.T., Lambeck, K., 1995. High-precision U-series dating of corals from Western Australia and implications for the timing and duration of the last interglacial. Earth Planet. Sci. Lett. 135, 115–130.
Suguio, K., Martin, L., 1981. Significance of Quaternary sea-level fluctuations for delta construction along the Brazilian Coast. Geo-Mar. Lett. 1, 181–185.
Suguio, K., Martin, L., Flexor, J.M., 1980. Sea-level fluctuations during the past 6,000 years along the coast of the State of São Paulo, Brazil. In: Mörner, N.A. (Ed.), Earth Rheology, Isostasy and Eustasy. John Willey and Sons, pp. 471–486.
Suguio, K., Martin, L., Dominguez, J.M.L., 1982. Evolução do "delta" do Rio Doce (ES) durante o Quaternário: influência das variações do nível do mar. 4°. Simpósio do Quaternário do Brasil. Sociedade Brasileira de Geologia, Rio de Janeiro, pp. 93–116.
Suguio, K., Martin, L., Bittencourt, A.C.S.P., Dominguez, J.M.L., Flexor, J.M., Azevedo, A.E.G., 1985. Flutuações do nível relativo do mar durante o Quaternário superior ao longo do litoral brasileiro e suas implicações na sedimentação costeira. Rev. Bras. Geosci. 15, 273–286.
Summerhayes, C.P., Melo, U., Barretto, H.T., 1976. The influence of upwelling on suspended matter and shelf sediments off southeastern Brazil. J. Sediment. Petrol. 6, 819–828.
Toscano, M.A., Lundberg, J., 1999. Submerged Late Pleistocene reefs on the tectonically-stable S.E. Florida margin: high-precision geochronology, stratigraphy, resolution of Substage 5a sea-level elevation, and orbital forcing. Quat. Sci. Rev. 18, 753–767.
USGS—United States Geological Survey, 2013. Image Catalog, EROS (Earth Resources Observation and Science Center). Available at, http://glovis.usgs.gov/ (Access in September 14th, 2013).
Valeriano, M.M., Kuplich, T.M., Storino, M., Amaral, B.D., Mendes, J.N., Lima Jr., D.J., 2006. Modeling small watersheds in Brazilian Amazonia with shuttle radar topographic mission-90 m data. Comput. Geosci. 32, 1169–1181.

Veeh, H.H., 2012. $Th^{230}/U^{238}$ and $U^{234}/U^{238}$ ages of Pleistocene high sea level stand. J. Geophys. Res. 71, 3379–3386.
Waelbroeck, C., Labeyrie, L., Michel, E., Duplessy, J.C., McManus, J.F., Lambeck, K., Balbon, E., Labracherie, M., 2002. Sea-level and deep water temperature changes derived from benthic foraminifera isotopic records. Quat. Sci. Rev. 21, 295–305.
Weise, B.R., 1980. Wave-dominated deltaic systems of the Upper Cretaceous San Miguel Formation, Maverick Basin, south Texas. Bulletin of the Economy Geology of the University of Texas, Austin 107 (39 pp.).
Wintle, A.G., Murray, A.S., 2006. A review of optically stimulated luminescence characteristic and their relevance in single-aliquot regeneration dating protocols. Radiat. Meas. 41, 369–391.